Supporting Information

Ringing the transformation associated with hydrazone changes of hexadecanuclear dysprosium phosphonates

Haiquan Tian,*[a] Fu-Ping Huang,[b] Yongfei Li,[a] Peiqiong Chen,[a] Keyu Chai,[a] Jing Lu,[a] Hou-Ting Liu,[a] Suyuan Zeng,[a] Dacheng Li[a] and Jianmin Dou[a]

[a]Shandong Provincial Key Laboratory of Chemical Energy Storage and Novel Cell Technology, School of Chemistry and Chemical Engineering, Liaocheng University, Liaocheng 252059, P. R. China. E-mail: tianhaiquan@lcu.edu.cn

[b]Key Laboratory for the Chemistry and Molecular Engineering of Medicinal Resources (Ministry of Education of China), School of Chemistry and Pharmacy, Guangxi Normal University, Guilin, 541004, P. R. China.

Table S1 Selected bond lengths (Å) and angles (º) for **1**.

Complex 1					
Dy1–O1	2.496(5)	Dy4–O19	2.402(5)	Dy8–O28a	2.562(5)
Dy1–O2	2.675(6)	Dy4–N6	2.476(6)	Dy8–N4	2.534(6)
Dy1–O22	2.260(5)	Dy5–O10	2.352(5)	Dy1···Dy2	3.780(9)
Dy1–O29	2.370(6)	Dy5–O16	2.259(6)	Dy1···Dy3	3.951(5)
Dy1–O30	2.378(6)	Dy5–O18	2.438(6)	Dy1···Dy7	4.053(6)
Dy1–O31	2.182(8)	Dy5–O23	2.281(5)	Dy2···Dy3	3.943(6)
Dy1–O32	2.294(7)	Dy5–O7a	2.375(6)	Dy2···Dy8	4.055(6)
Dy1–N16	2.502(8)	Dy5–O12a	2.446(5)	Dy4···Dy5	4.385(5)
Dy2–O1	2.489(6)	Dy5–O14a	2.549(5)	Dy4···Dy6	4.029(5)
Dy2–O3	2.577(5)	Dy6–O12	2.351(5)	Dy5···Dy6	3.983(8)
Dy2–O25	2.444(6)	Dy6–O17	2.413(6)	Dy5···Dy7	3.888(2)
Dy2–O26	2.350(6)	Dy6–O19	2.414(5)	Dy6···Dy8	4.037(6)
Dy2–O29	2.355(4)	Dy6–O20	2.195(6)	Dy7···Dy8	3.906(3)
Dy2–O33	2.338(8)	Dy6–O28	2.287(5)	Dy4···Dy6a	5.820(3)
Dy2–O34	2.501(7)	Dy6–O10a	2.431(5)	Dy5···Dy6a	3.983(2)
Dy2–O2w	2.418(7)	Dy6–O11a	2.589(5)	Dy4···Dy4a	6.251(6)
Dy2–N14	2.627(9)	Dy6–N8	2.510(6)	Dy1–O1–Dy2	98.6(2)
Dy3–O21	2.375(5)	Dy7–O2	2.291(5)	Dy1–O2–Dy7	107.3(2)
Dy3–O24	2.230(5)	Dy7–O4	2.363(6)	Dy1–O29–Dy2	106.2(2)
Dy3–O25	2.359(6)	Dy7–O6	2.373(6)	Dy1–O29–Dy3	112.3(2)
Dy3–O27	2.293(7)	Dy7–O8	2.284(5)	Dy2–O29–Dy3	112.5(2)
Dy3–O29	2.388(5)	Dy7–O14	2.261(5)	Dy1–O30–Dy3	113.0(2)
Dy3–O30	2.362(7)	Dy7–O22a	2.485(5)	Dy2–O3–Dy8	110.4(2)
Dy3–N10	2.645(13)	Dy7–O23a	2.532(5)	Dy4–O18–Dy5	124.7(2)
Dy3–N11	2.543(8)	Dy7–N2	2.561(9)	Dy4–O19–Dy6	113.6(2)
Dy4–O1w	2.340(5)	Dy8–O3	2.359(5)	Dy5–O12–Dy6	112.3(2)
Dy4–O9	2.203(7)	Dy8–O4	2.374(6)	Dy5–O10–Dy6a	112.8(2)
Dy4–O13	2.429(5)	Dy8–O5	2.261(6)	Dy5–O14–Dy7a	107.7(2)
Dy4–O15	2.314(6)	Dy8–O8	2.333(6)	Dy6–O11–Dy8a	111.2(1)
Dy4–O17	2.419(5)	Dy8–O11	2.302(5)	Dy7–O4–Dy8	111.1(2)
Dy4–O18	2.512(5)	Dy8–O26a	2.509(6)	Dy7–O8–Dy8	115.6(2)

Symmetry code: a: 1-x, 1-y, 1-z.

Table S2 Selected bond lengths (Å) and angles (º) for **2**.

Complex 2					
Dy1–O2	2.233(19)	Dy3–O19	2.369(19)	Dy2···Dy4	5.171(2)
Dy1–O6	2.222(19)	Dy3–O20	2.231(19)	Dy3···Dy4	5.449(2)
Dy1–O7	2.258(58)	Dy3–O22	2.360(20)	Dy4···Dy4a	5.912(7)
Dy1–O10	2.213(19)	Dy3–N3	2.530(30)	Dy4···Dy4b	8.360(5)
Dy1–O18	2.364(19)	Dy3–O3a	2.220(19)	Dy1···Dy1a	9.975(2)
Dy1–O24	2.330(20)	Dy4–O5	2.267(19)	Dy1···Dy1b	13.437(3)
Dy2–O9	2.209(19)	Dy4–O8	2.200(19)	Dy2···Dy2a	12.672(8)
Dy2–O12	2.240(20)	Dy4–O16	2.238(16)	Dy2···Dy2b	17.899(5)
Dy2–O13	2.260(20)	Dy4–O23	2.415(19)	Dy3···Dy3a	13.622(2)
Dy2–O17	2.399(17)	Dy4–O1a	2.226(19)	Dy3···Dy3b	18.952(8)
Dy2–O18	2.438(19)	Dy4–O4a	2.202(16)	Dy1–O18–Dy2	122.0(8)
Dy2–O19	2.322(19)	Dy1···Dy2	4.200(4)	Dy2–O17–Dy3	107.7(7)
Dy2–N1	2.540(30)	Dy1···Dy3	4.906(8)	Dy2–O19–Dy3	111.6(7)
Dy3–O14	2.284(19)	Dy1···Dy3	7.101(2)		
Dy3–O17	2.407(16)	Dy2···Dy3	3.879(7)		
Symmetry code: a: 0.5-x, 0.5-y, z; b: y, 0.5-x, 1.5-z.					

Table S3 Dy^{III} geometry analysis of **1** and **2** by SHAPE 2.1 software.

Complex 1									
Geometry (CN = 7)	**Dy5**	**Geometry (CN = 8)**	**Dy1**	**Dy3**	**Dy4**	**Dy6**	**Dy7**	**Dy8**	**Geometry (CN = 9)**	**Dy2**
CTPR-7	3.462	**JBTPR-8**	2.071	27.865	4.237	3.417	25.910	26.349	**JCSAPR-9**	22.535
PBPY-7	4.004	**BTPR-8**	2.474	25.515	3.189	3.168	26.311	28.000	**JTCTPR-9**	22.565
COC-7	5.735	**JSD-8**	2.965	29.383	5.135	3.134	26.728	27.460	**CSAPR-9**	22.819
JPBPY-7	7.180	**TDD-8**	3.460	25.614	2.060	3.486	26.608	27.399	**TCTPR-9**	22.994
HPY-7	17.965	**SAPR-8**	3.644	27.519	4.574	4.685	26.664	28.893	**MFF-9**	23.063
JETPY-7	18.427	**JGBF-8**	8.690	27.350	12.653	9.037	31.380	32.964	**JTC-9**	26.971
HP-7	26.805	**CU-8**	9.422	31.963	7.576	9.156	31.317	32.354	**HH-9**	27.863
		TT-8	9.872	31.201	8.154	9.963	29.814	30.662	**CCU-9**	28.000
		HBPY-8	11.510	31.987	11.578	11.028	31.312	30.274	**JCCU-9**	28.046
		ETBPY-8	20.871	39.036	23.359	21.272	39.473	39.626	**JTDIC-9**	29.310
		JETBPY-8	23.616	40.257	26.583	23.318	42.393	43.318	**HBPY-9**	34.395
		HPY-8	24.322	35.727	22.955	24.626	37.838	38.770	**OPY-9**	36.599
		OP-8	29.969	47.533	35.234	32.260	47.328	48.711	**EP-9**	45.789

Complex 2					
Geometry (CN = 6)	**Dy1**	**Dy4**	**Geometry (CN = 7)**	**Dy2**	**Dy3**
HP-6	50.552	49.337	**HP-7**	42.993	44.176
PPY-6	33.841	33.439	**HPY-7**	27.907	28.449
OC-6	30.303	29.961	**PBPY-7**	27.496	25.863
TPR-6	39.456	39.673	**COC-7**	28.911	30.255
JPPY-6	38.499	37.721	**CTPR-7**	27.415	29.162
			JPBPY-7	22.403	20.724
			JETPY-7	35.013	38.132

Lable	**Shape**	**Lable**	**Shape**	**Lable**	**Shape**	**Lable**	**Shape**	**Lable**	**Shape**
HP-6	Hexagon (D_{6h})	COC-7	Capped octahedron (C_{3v})	SAPR-8	Square antiprism (D_{4d})	ETBPY-8	Elongated trigonal bipyramid (D_{3h})	CSAPR-9	Spherical capped square antiprism (C_{4v})
PPY-6	Pentagonal pyramid (C_{5V})	CTPR-7	Capped trigonal prism (C_{2v})	TDD-8	Triangular dodecahedron (D_{2d})	EP-9	Enneagon (D_{9h})	JTCTPR-9	Tricapped trigonal prism J51 (D_{3h})
OC-6	Octahedron (O_h)	JPBPY-7	Johnson pentagonal bipyramid J13 (D_{5h})	JGBF-8	Johnson gyrobifastigium J26 (D_{2d})	OPY-9	Octagonal pyramid (C_{8v})	TCTPR-9	Spherical tricapped trigonal prism (D_{3h})
TPR-6	Trigonal prism (D_{3h})	JETPY-7	Elongated triangular pyramid J7 (C_{3v})	JETBPY-8	Johnson elongated triangular bipyramid J14 (D_{3h})	HBPY-9	Heptagonal bipyramid (D_{7h})	JTDIC-9	Tridiminished icosahedron J63 (C_{3v})
JPPY-5	Johnson pentagonal pyramid (C_{5V})	OP-8	Octagon	JBTPR-8	Biaugmented trigonal prism J50 (C_{2v})	JTC-9	Johnson triangular cupola J3 (C_{3v})	HH-9	Hula-hoop (C_{2v})
HP-7	Heptagon	HPY-8	Heptagonal pyramid (C_{7v})	BTPR-8	Biaugmented trigonal prism (C_{2v})	JCCU-9	Capped cube J8 (C_{4v})	MFF-9	Muffin (C_s)
HPY-7	Hexagonal pyramid (C_{6v})	HBPY-8	Hexagonal bipyramid (D_{6h})	JSD-8	Snub diphenoid J84 (D_{2d})	CCU-9	Spherical-relaxed capped cube (C_{4v})		
PBPY-7	Pentagonal bipyramid (D_{5h})	CU-8	Cube (O_h)	TT-8	Triakis tetrahedron (T_d)	JCSAPR-9	Capped square antiprism J10 (C_{4v})		

Table S4 Relaxation fitting parameters from least-squares fitting of $\chi(\omega)$ data under zero *dc* field for **1**.

T	χ_T	χ_s	α	$\ln(\tau / s)$
1.8	95.58	54.42	0.289	-9.190
2.0	82.23	48.77	0.281	-9.073
2.3	70.05	40.95	0.240	-9.074
2.6	59.07	32.93	0.215	-9.138
2.9	49.26	25.74	0.195	-9.193
3.2	39.72	18.28	0.184	-9.270
3.5	30.41	10.59	0.177	-9.363
3.7	22.04	3.96	0.171	-9.433
4.0	15.36	-1.36	0.170	-9.528
4.5	10.00	-4.00	0.165	-9.646
5.0	4.34	-7.34	0.167	-9.778
5.5	-0.44	-10.56	0.179	-9.980
6.0	-2.15	-10.85	0.193	-10.196
6.5	-4.33	-11.67	0.207	-10.397
7.0	-6.20	-12.80	0.238	-10.746
7.5	-7.78	-15.22	0.285	-11.521
8.0	-8.94	-16.06	0.319	-12.055

Table S5 Relaxation fitting parameters from least-squares fitting of $\chi(\omega)$ data under 1.0 kOe *dc* field for **1**.

T	χ_T	χ_s	α	$\ln(\tau / s)$
1.8	99.96	44.04	0.309	-7.767
2.0	79.00	34.00	0.294	-7.763
2.3	66.79	30.21	0.283	-7.775
2.6	53.82	22.18	0.250	-7.813
2.9	41.51	13.49	0.230	-7.85
3.2	31.18	5.82	0.219	-7.896
3.5	22.92	0.08	0.205	-7.926
3.7	15.76	-4.76	0.190	-7.951
4.0	10.81	-7.81	0.180	-7.987
4.5	6.26	-9.26	0.161	-8.028
5.0	2.43	-10.43	0.141	-8.072
5.5	0.39	-10.39	0.130	-8.149
6.0	-1.55	-10.45	0.117	-8.219
6.5	-3.34	-10.66	0.107	-8.294
7.0	-5.11	-10.89	0.087	-8.552
7.5	-6.14	-10.86	0.084	-8.893
8.0	-7.10	-10.90	0.079	-9.253
8.5	-8.09	-10.90	0.055	-9.792
9.0	-8.90	-11.10	0.060	-10.336
9.5	-9.66	-11.34	0.057	-10.868
10.0	-10.38	-11.62	0.044	-11.292
10.5	-11.07	-11.93	0.018	-11.629

Table S6 Relaxation fitting parameters from least-squares fitting of $\chi(\omega)$ data under zero *dc* field for **2**.

T	χ_T	χ_s	α	$\ln(\tau / s)$
1.8	78.95	61.05	0.481	-9.366
2.0	75.35	59.65	0.485	-9.401
2.3	71.62	56.37	0.510	-9.426
2.6	68.55	55.45	0.516	-9.470
2.9	63.83	51.17	0.522	-9.608
3.2	61.59	48.41	0.526	-9.735
3.5	59.06	46.94	0.525	-9.820
3.7	56.72	45.28	0.531	-9.902
4.0	54.89	44.11	0.530	-10.054
4.5	52.86	43.14	0.536	-10.306
5.0	50.71	41.29	0.551	-10.624
5.5	49.64	39.36	0.590	-11.063
6.0	49.19	36.81	0.620	-11.667
6.5	47.48	35.52	0.624	-12.277
7.0	44.28	33.72	0.599	-12.617
7.5	47.03	27.97	0.627	-12.964
8.0	38.57	26.43	0.592	-13.208

Table S7 Relaxation fitting parameters from least-squares fitting of $\chi(\omega)$ data under 1.0 kOe *dc* field for **2**.

T	χ_T	χ_s	α	$\ln(\tau / s)$
1.8	33.82	16.18	0.533	-10.413
2.0	31.32	12.68	0.643	-10.428
2.3	29.02	10.98	0.526	-10.446
2.6	20.75	9.25	0.429	-10.460
2.9	21.44	8.56	0.477	-10.491
3.2	20.66	9.34	0.461	-10.529
3.5	21.05	8.95	0.480	-10.579
3.7	18.93	6.07	0.502	-10.615
4.0	18.25	3.75	0.533	-10.665
4.5	17.02	4.98	0.507	-10.725
5.0	15.62	3.38	0.515	-10.799
5.5	13.56	2.22	0.508	-10.860
6.0	11.10	1.37	0.480	-10.924
6.5	10.02	0.52	0.475	-11.051
7.0	9.40	-0.32	0.470	-11.107
7.5	6.86	-0.34	0.433	-11.249
8.0	9.99	-5.38	0.494	-11.447
8.5	8.85	-6.89	0.485	-11.690
9.0	8.82	-8.55	0.449	-11.857
9.5	5.97	-8.85	0.470	-12.097
10.0	5.38	-11.77	0.425	-12.216
10.5	4.57	-12.53	0.406	-12.493
11.0	4.37	-14.12	0.368	-12.640
12.0	4.30	-16.55	0.329	-12.840
13.0	5.63	-19.16	0.263	-13.035
14.0	4.41	-20.57	0.254	-13.232
15.0	6.19	-24.05	0.184	-13.454
16.0	12.45	-30.49	0.098	-13.641
17.0	14.39	-32.07	0.109	-13.825
18.0	21.28	-39.74	0.116	-14.036
19.0	24.27	-39.18	0.118	-14.162

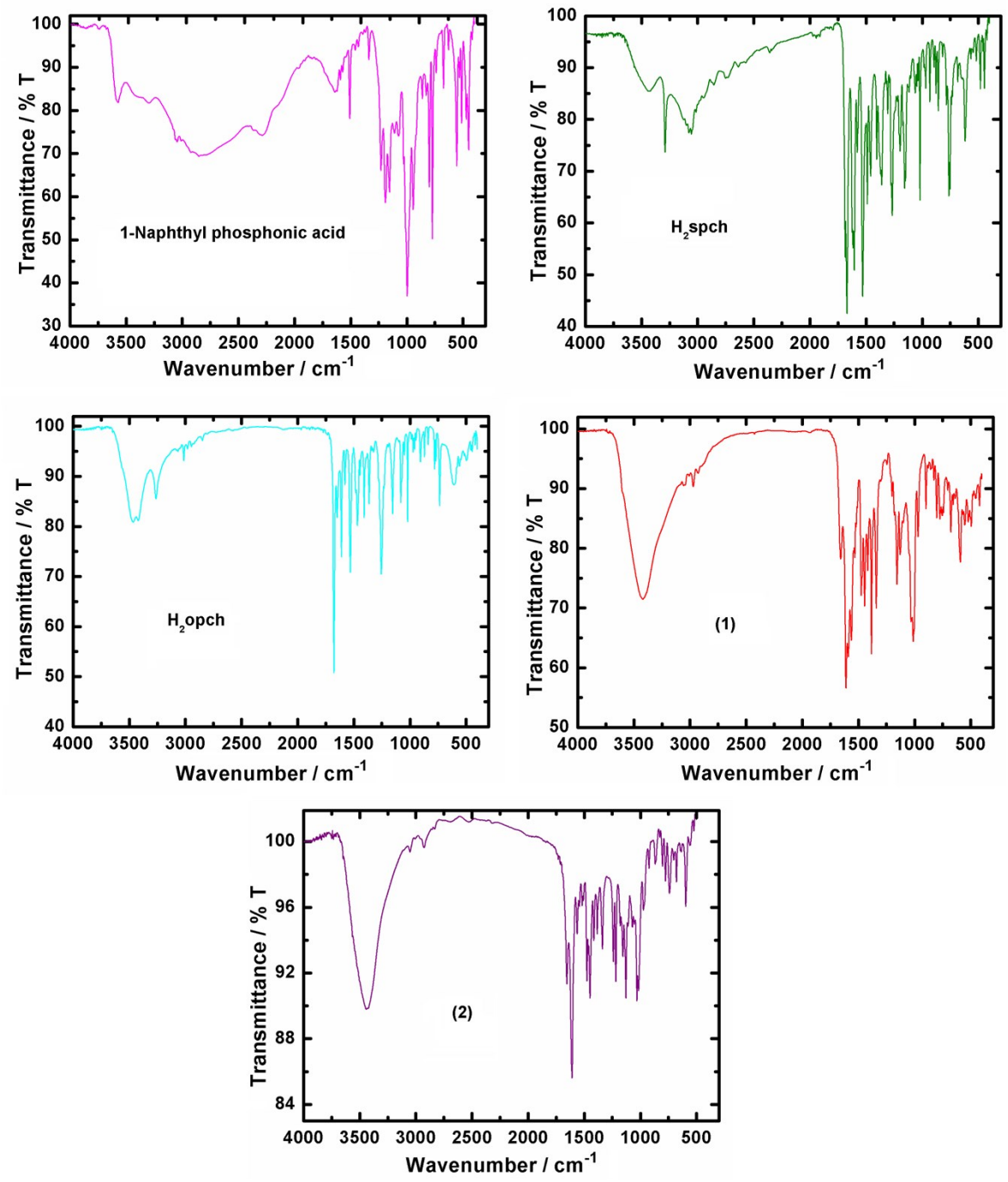

Figure S1 Infrared spectra of **1-naphthylphosphonic acid**, **H_2spch**, **H_2opch**, **1** and **2**.

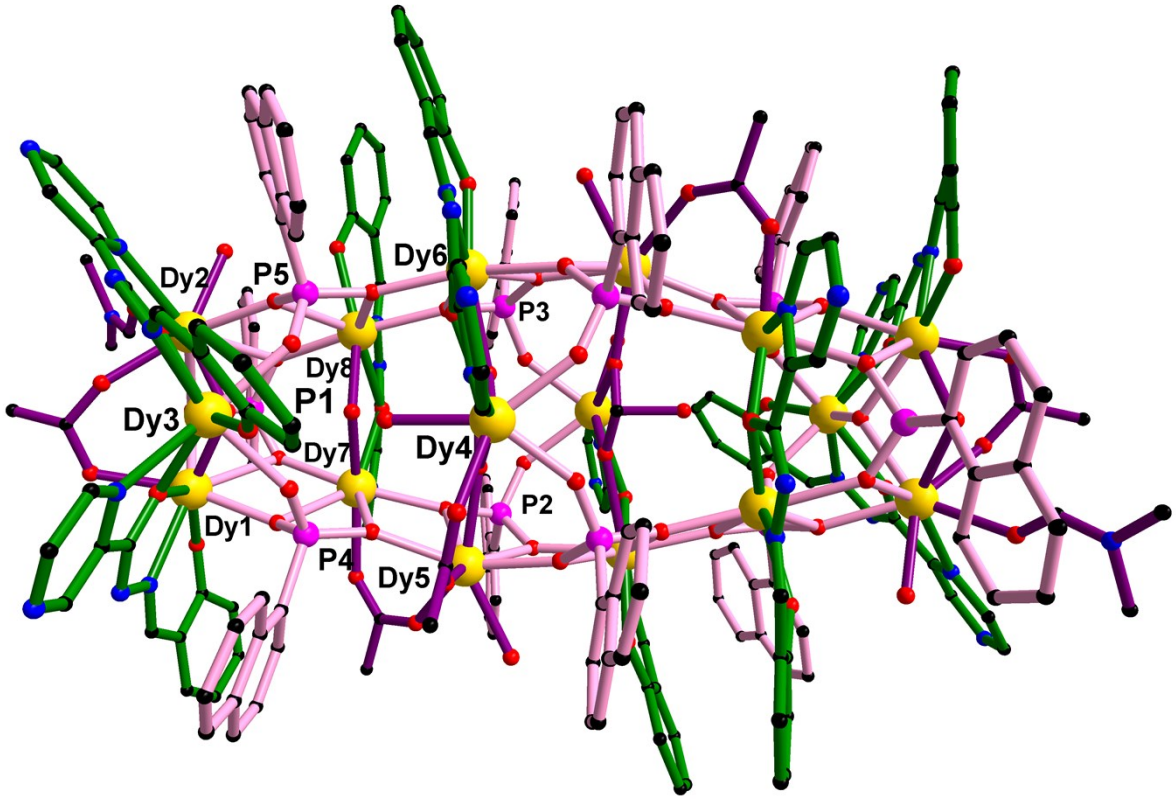

Figure S2 Partially labeled structure of **1**. The $spch^{2-}$ fragments are shown in green, the $C_{10}H_7PO_3$ in rose, Dy in gold, O in red, N in blue, P in pink.

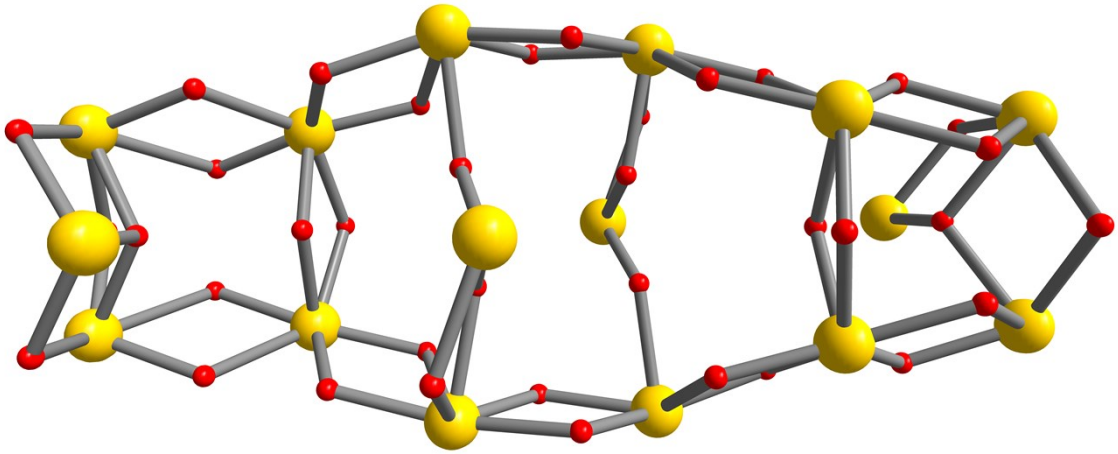

Figure S3 The Dy_{16} core of **1**. Color code: Dy in gold, O in red.

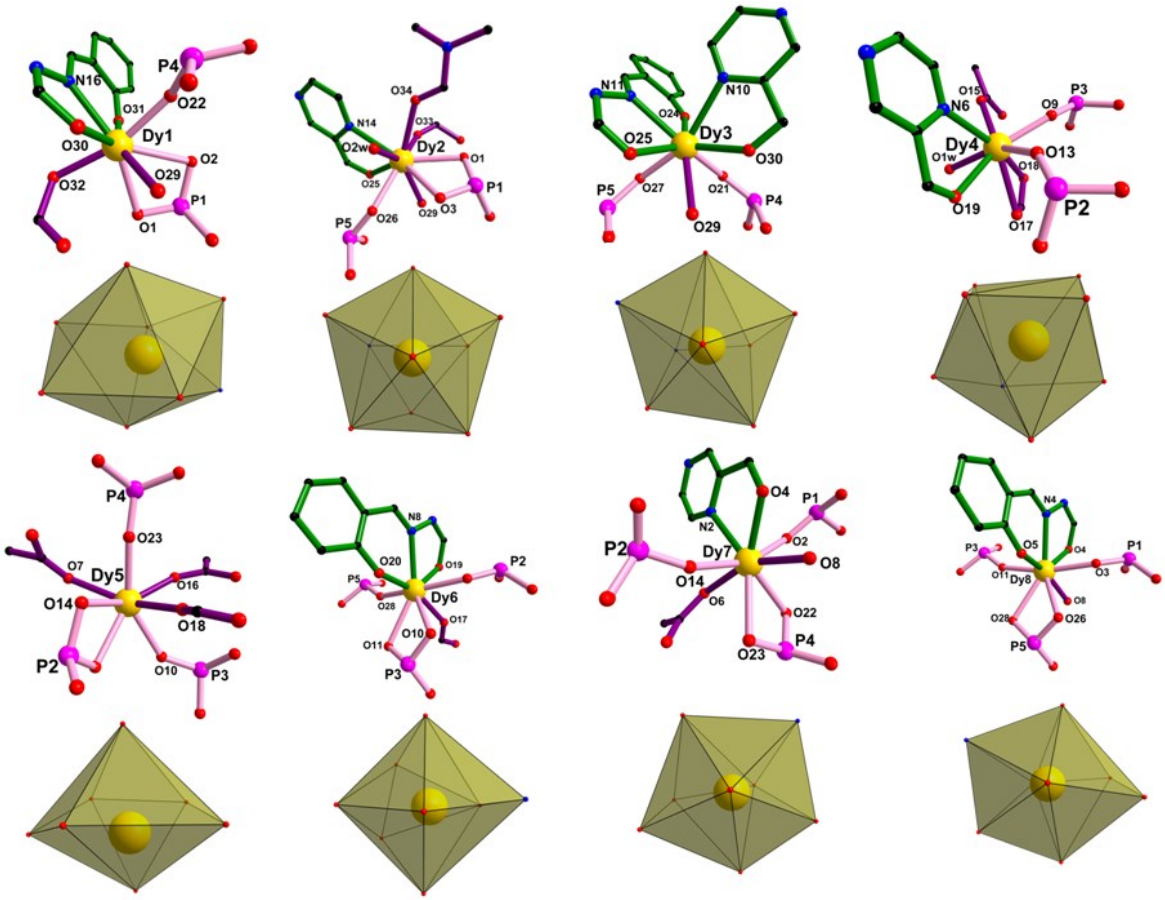

Figure S4 Coordination environments of eight crystallographically independent Dy ions in **1**. The $spch^{2-}$ fragments are shown in green, the PO_3^{2-} in rose, Dy in gold, O in red, N in blue, P in pink.

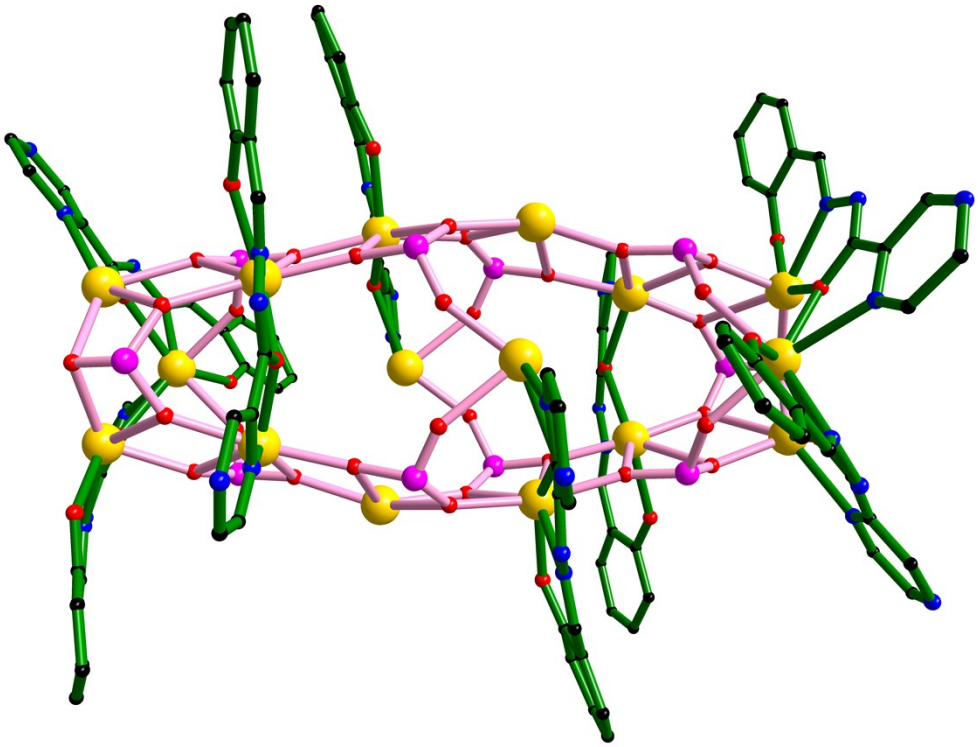

Figure S5 The $[Dy_{16}(spch)_8(PO_3)_{10}]^{12+}$ core for **1**. The $spch^{2-}$ fragments are shown in green, the PO_3^{2-} in rose, Dy in gold, O in red, N in blue, P in pink.

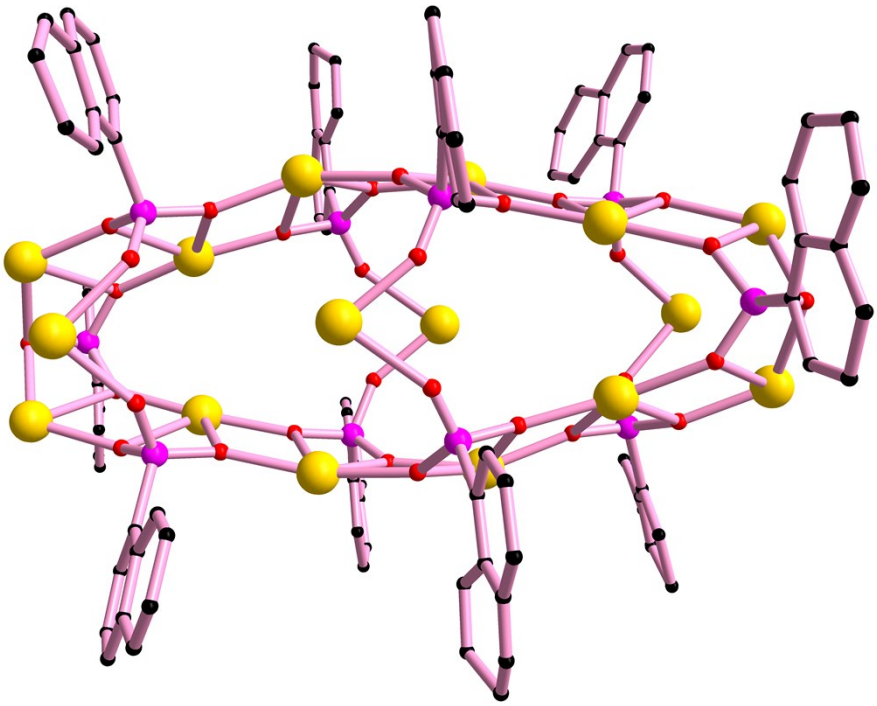

Figure S6 The $[Dy_{16}(C_{10}H_7\text{-}PO_3)_{10}]^{28+}$ core for **1**. Color code: the $C_{10}H_7PO_3$ in rose, Dy in gold, O in red, P in pink.

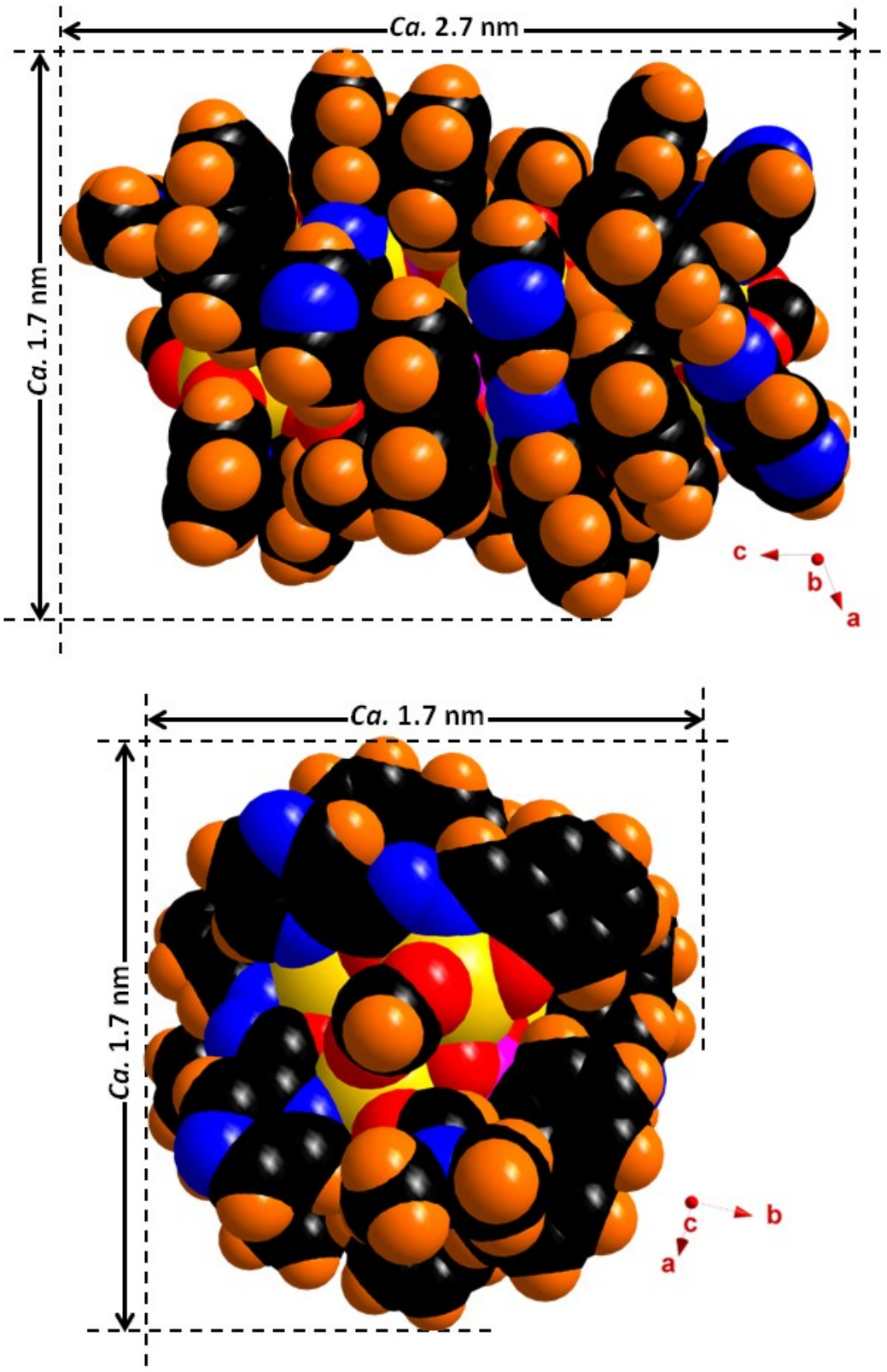

Figure S7 Space-filling representation exhibiting the longest (top) and shortest (bottom) diameters of **1**. Color code: Dy in gold, O in red, P in pink, H in orange.

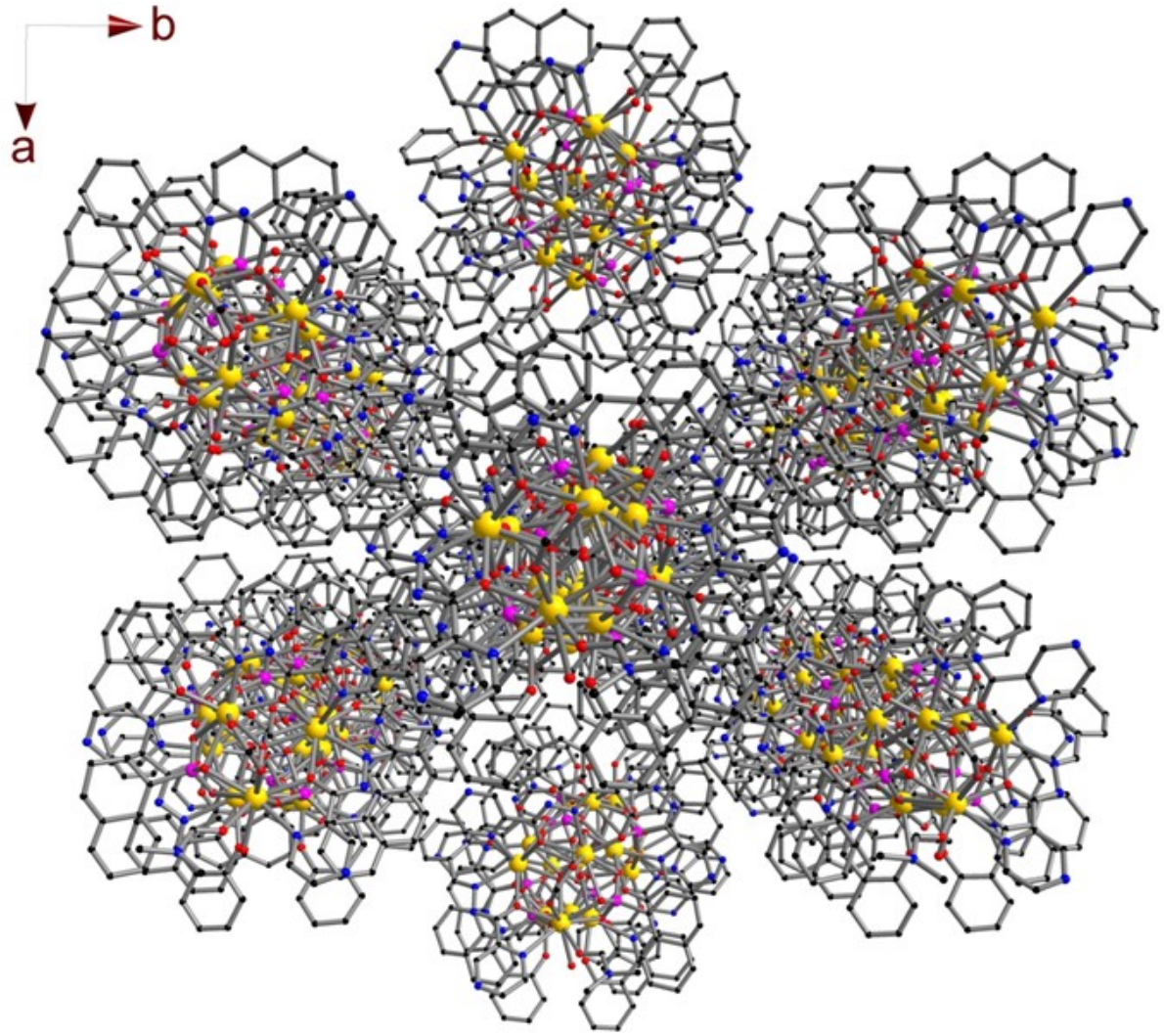

Figure S8 The molecular packing viewed along the *c* axis in **1**.

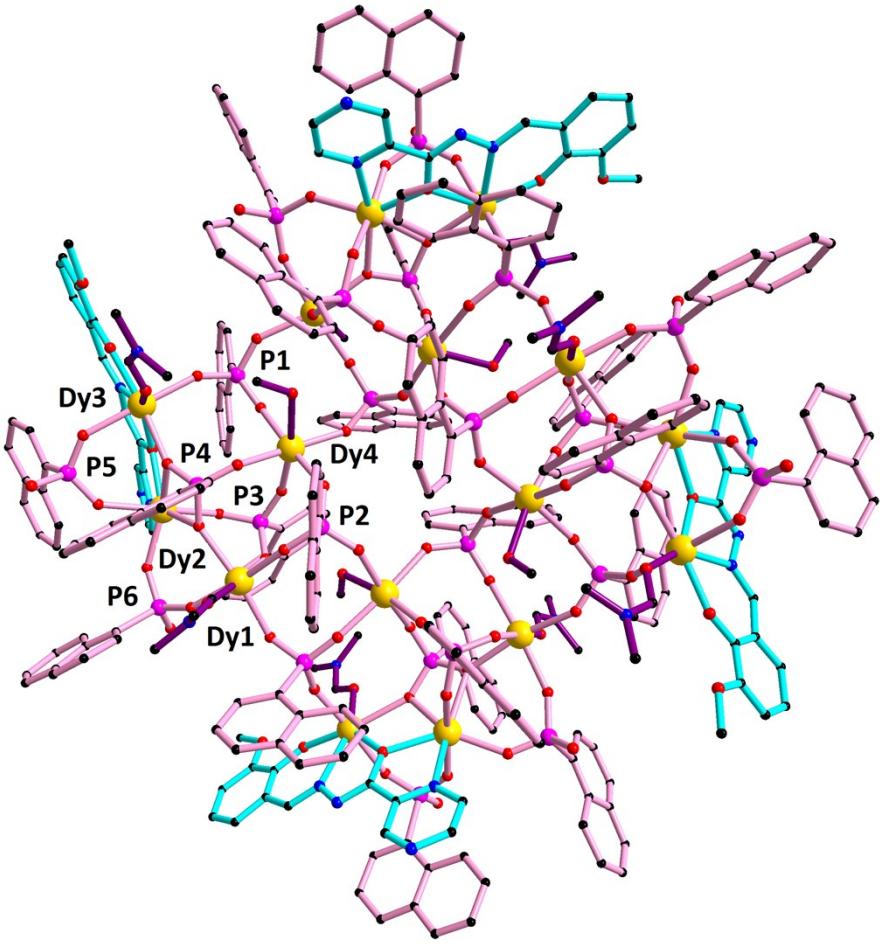

Figure S9 Partially labeled structure of **2**. The $opch^{2-}$ fragments are shown in turquoise, the $C_{10}H_7PO_3$ in rose, Dy in gold, O in red, N in blue, P in pink.

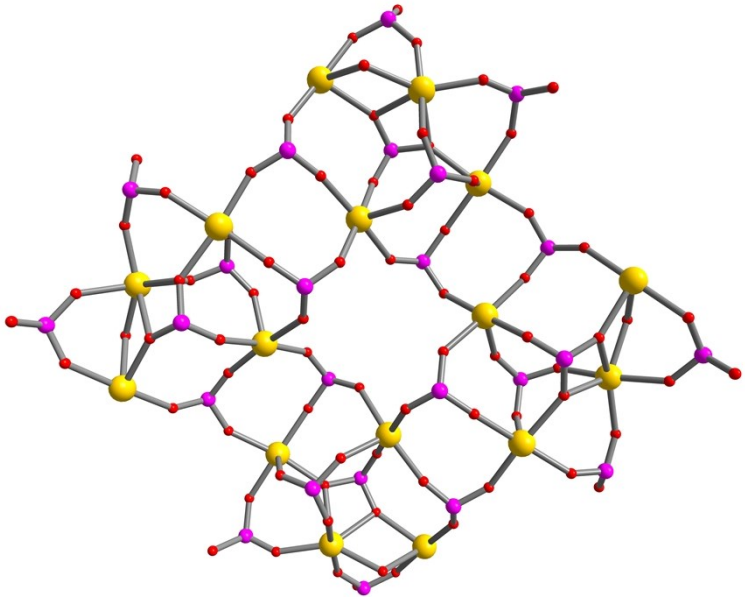

Figure S10 The Dy_{16} core of **2**. Color code: Dy in gold, O in red, P in pink.

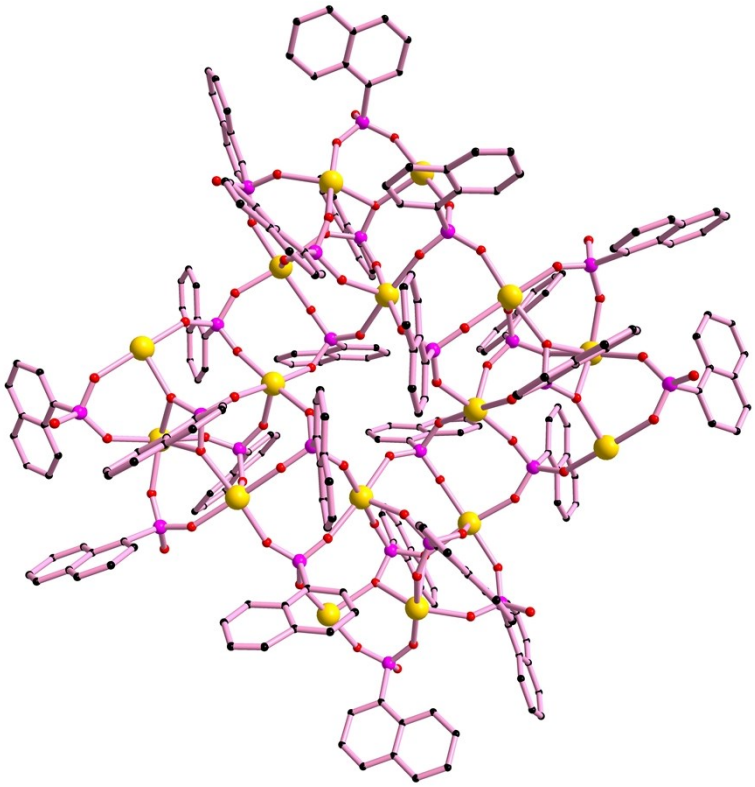

Figure S11 The $[Dy_{16}(C_{10}H_7\text{-}PO_3)_{24}]^{8+}$ core for **2**. Color code: the $C_{10}H_7PO_3$ in rose, Dy in gold, O in red, P in pink.

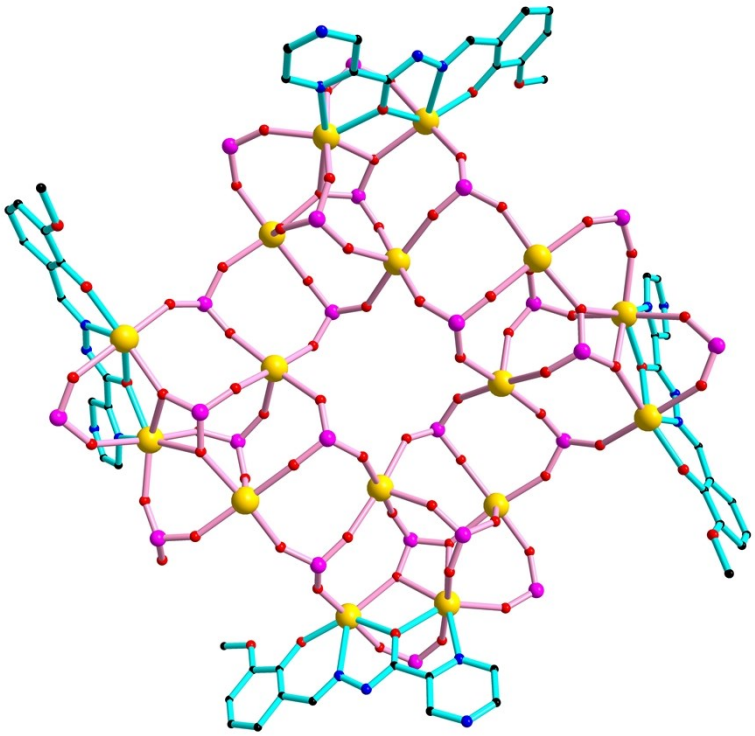

Figure S12 The $[Dy_{16}(spch)_8(PO_3)_{10}]^{12+}$ core for **2**. The $opch^{2-}$ fragments are shown in turquoise, the PO_3^{2-} in rose, Dy in gold, O in red, N in blue, P in pink.

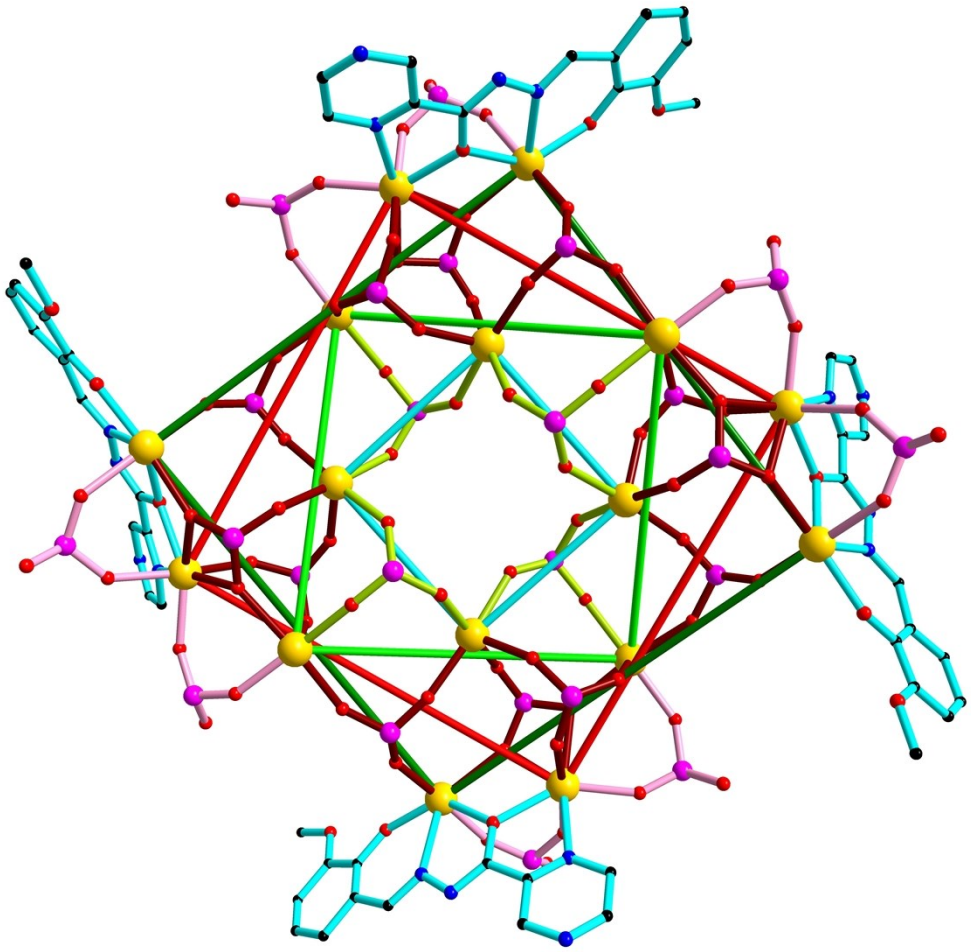

Figure S13 The turquoise, bright green, red and green squares denote square-within-square-within-square planar structures in **2**.

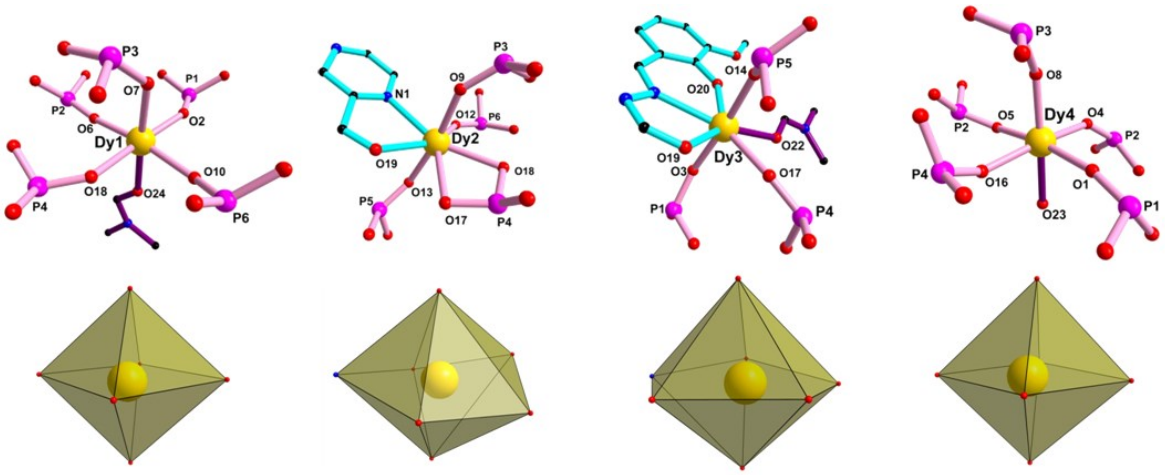

Figure S14 Coordination environments of four crystallographically independent Dy ions in **2**. The opch^{2-} fragments are shown in turquoise, the PO_3^{2-} in rose, Dy in gold, O in red, N in blue, P in pink.

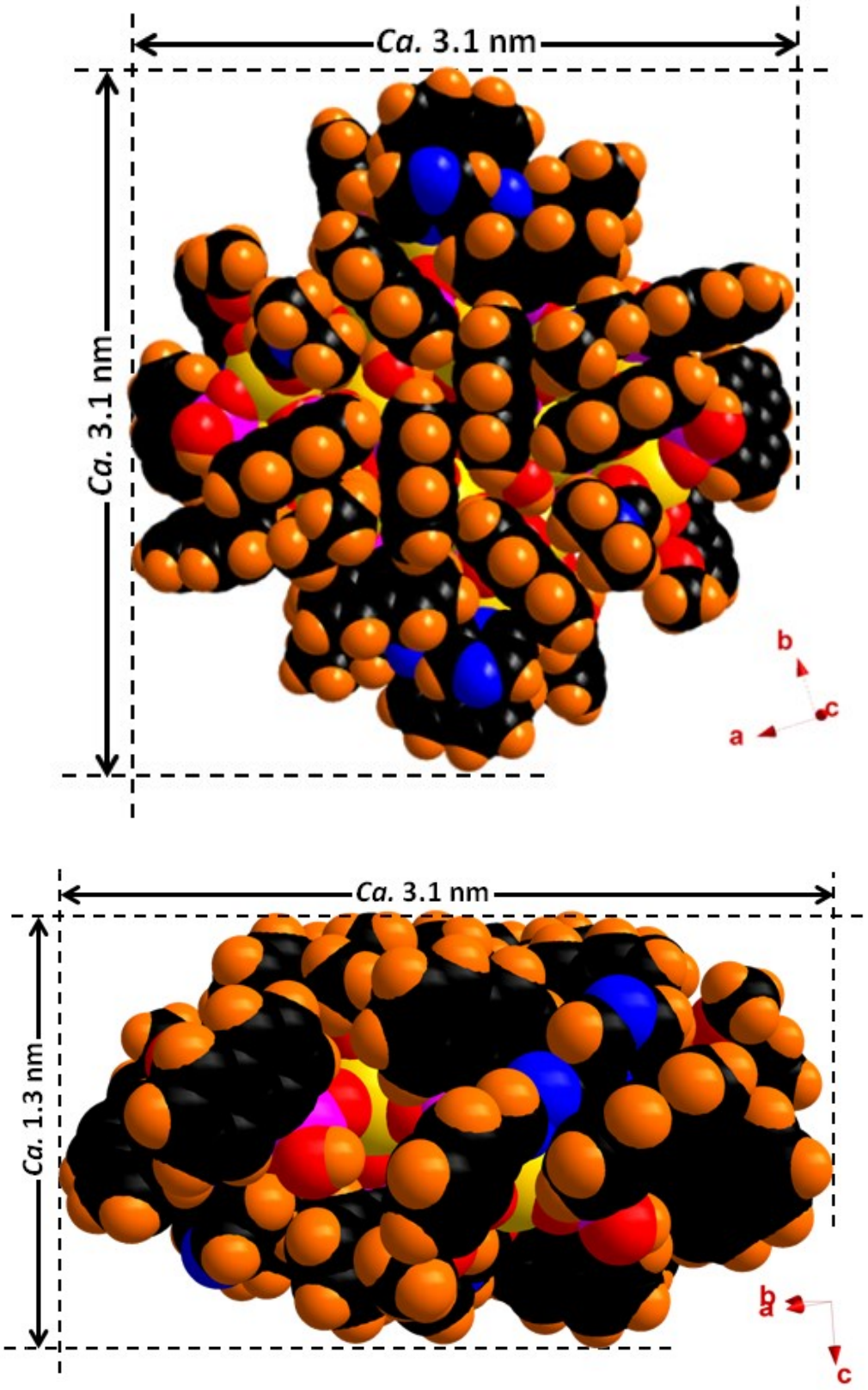

Figure S15 Space-filling representation exhibiting outer diameter (top) and thickness (bottom) of **2**. Color code: Dy in gold, O in red, P in pink, H in orange.

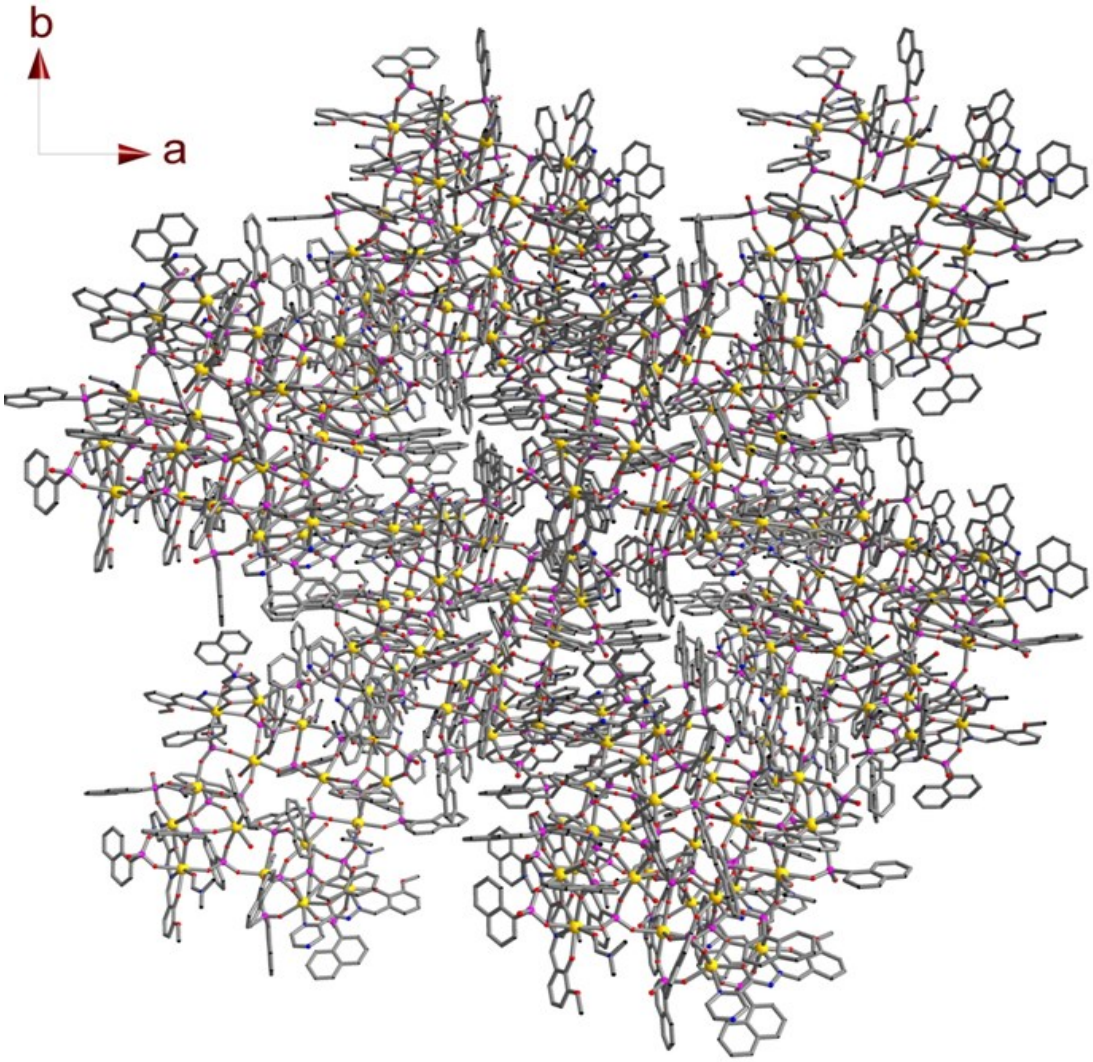

Figure S16 The molecular packing viewed along the *c* axis in **2**.

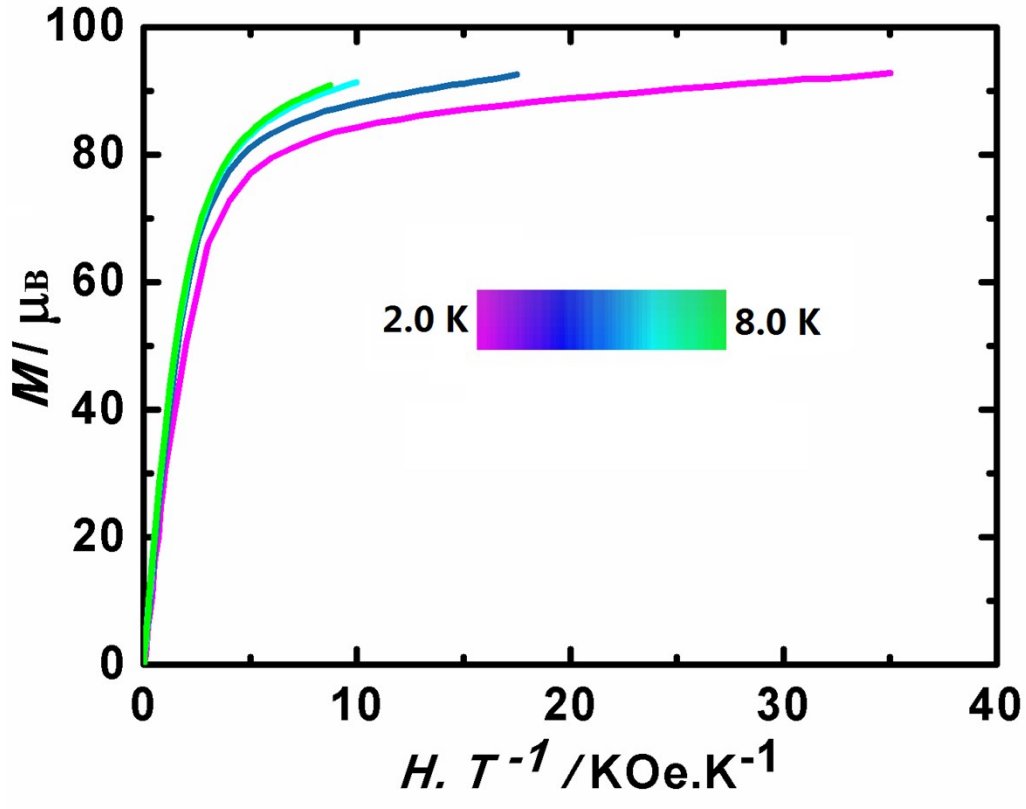

Figure S17 *M vs. H/T* plot for **1** at temperature range of 2.0 K – 8.0 K.

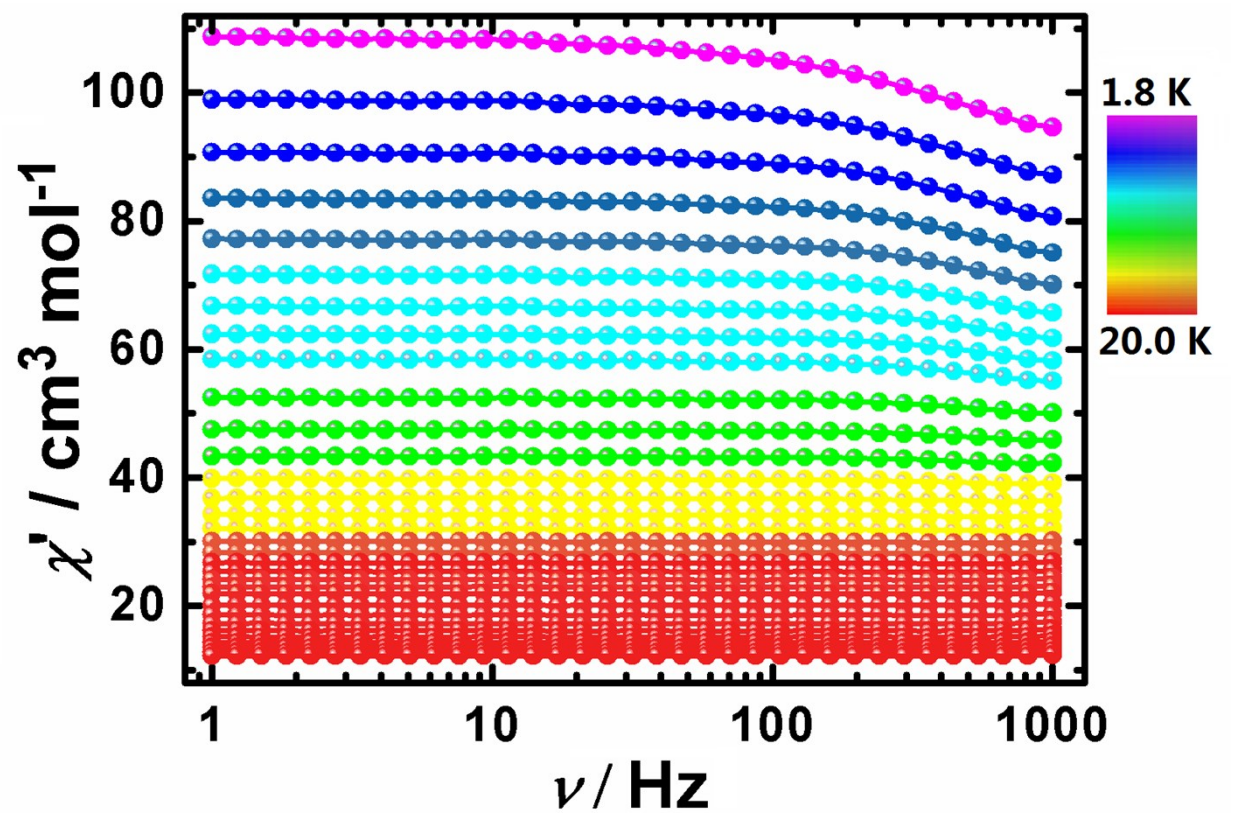

Figure S18 Frequency dependence of the χ' product, *ac* susceptibilities under zero *dc* field for **1**.

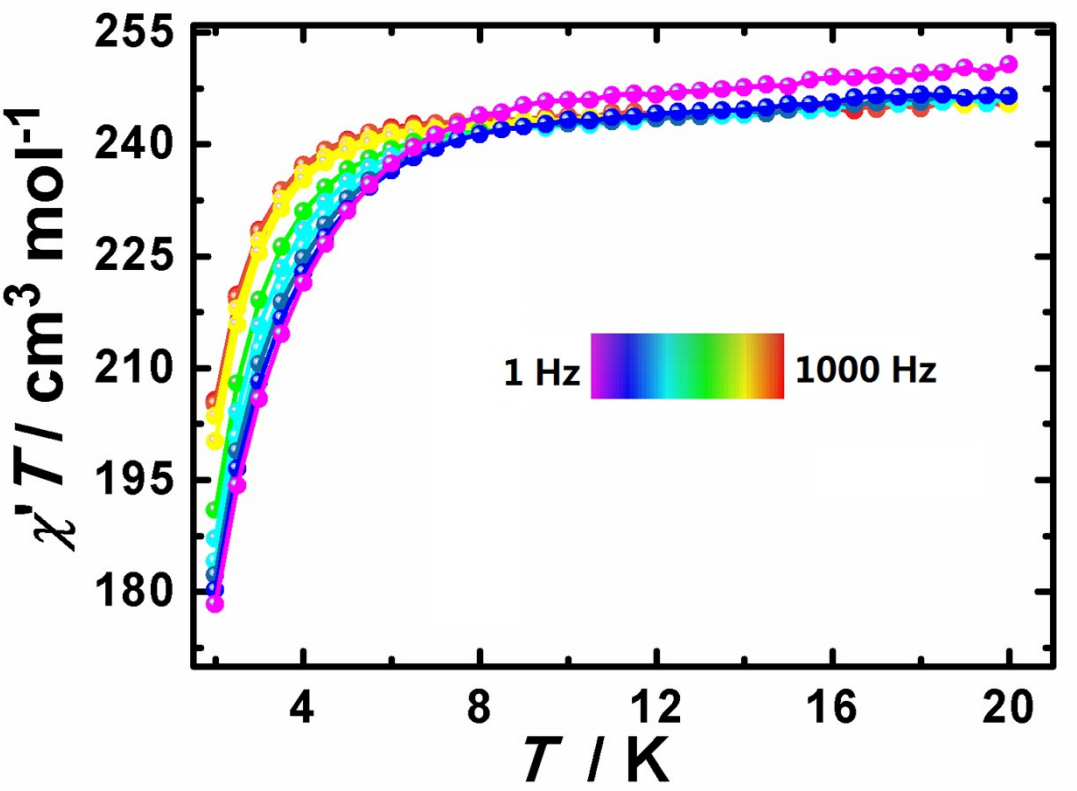

Figure S19 Frequency dependence of the $\chi'T$ product, *ac* susceptibilities under zero *dc* field for **1**.

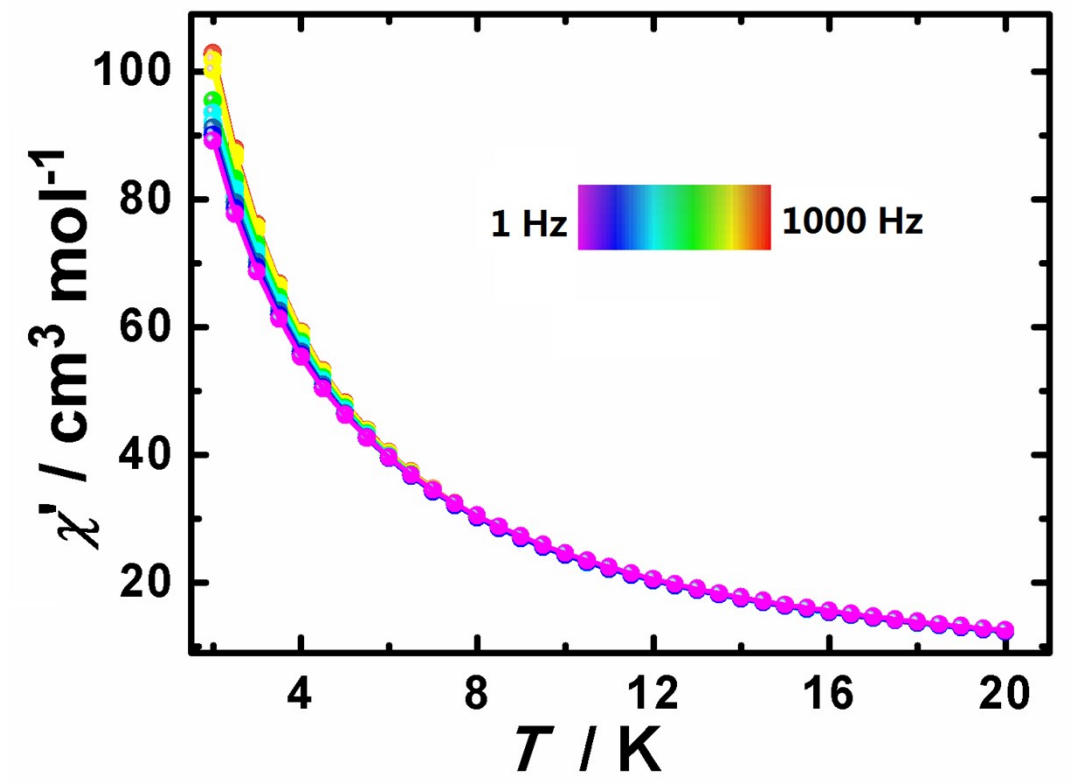

Figure S20 Temperature dependence of the χ' product, *ac* susceptibilities under zero *dc* field for **1**.

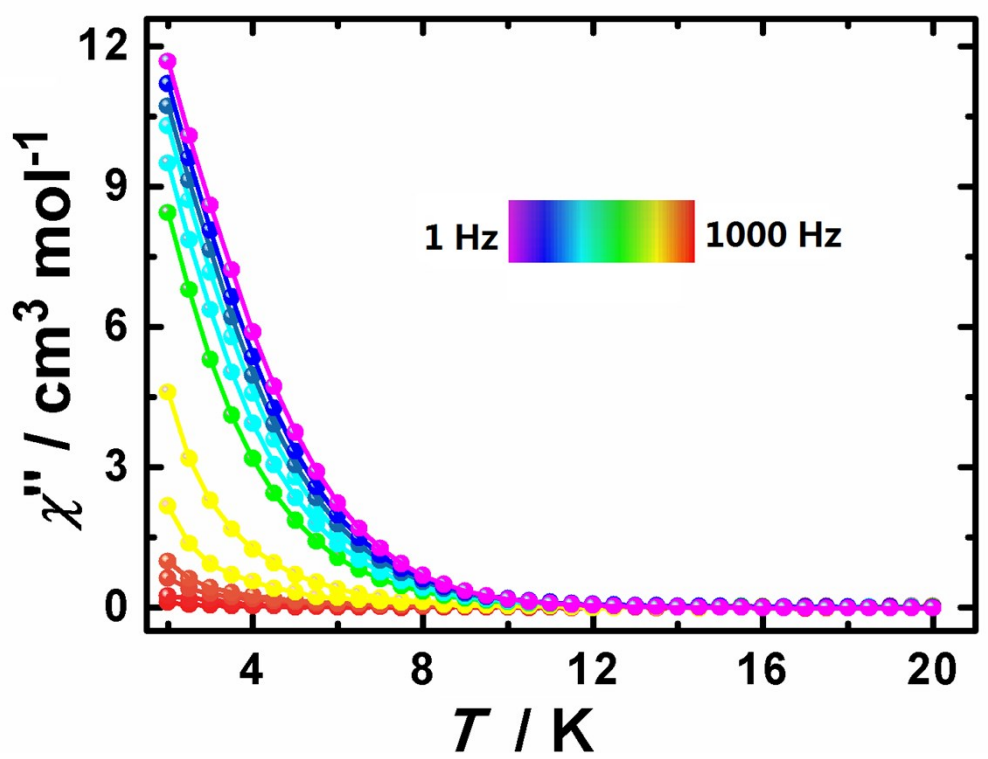

Figure S21 Temperature dependence of the χ'' product, *ac* susceptibility under zero *dc* field for **1**.

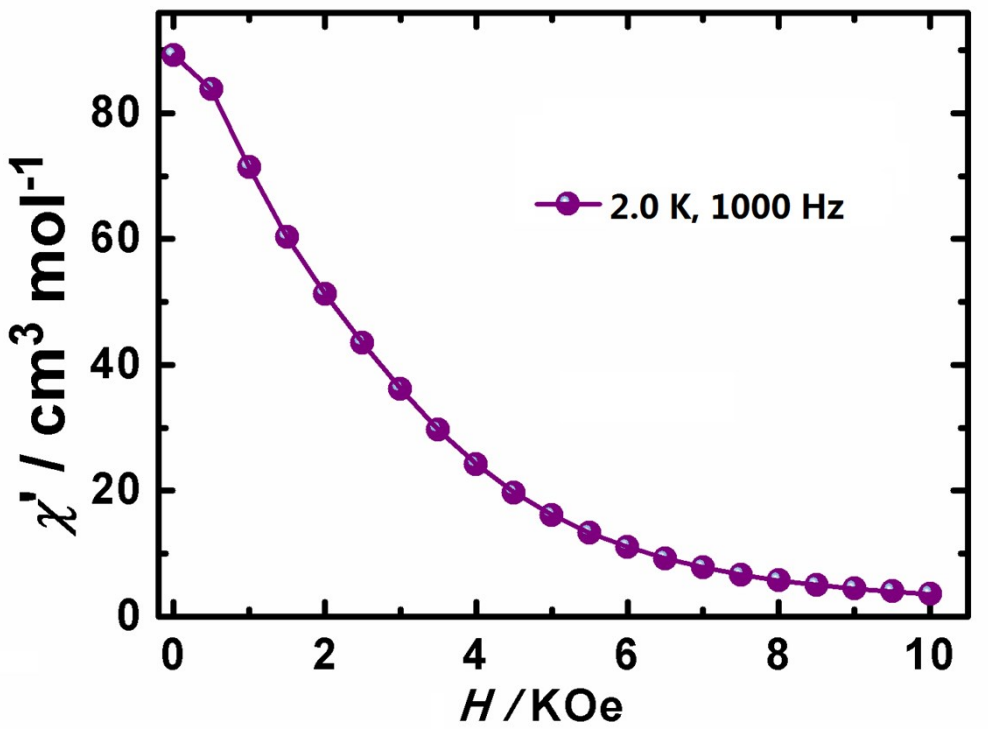

Figure S22 Field dependence of the χ' product, ac susceptibility of **1** at 1000 Hz and 2 K.

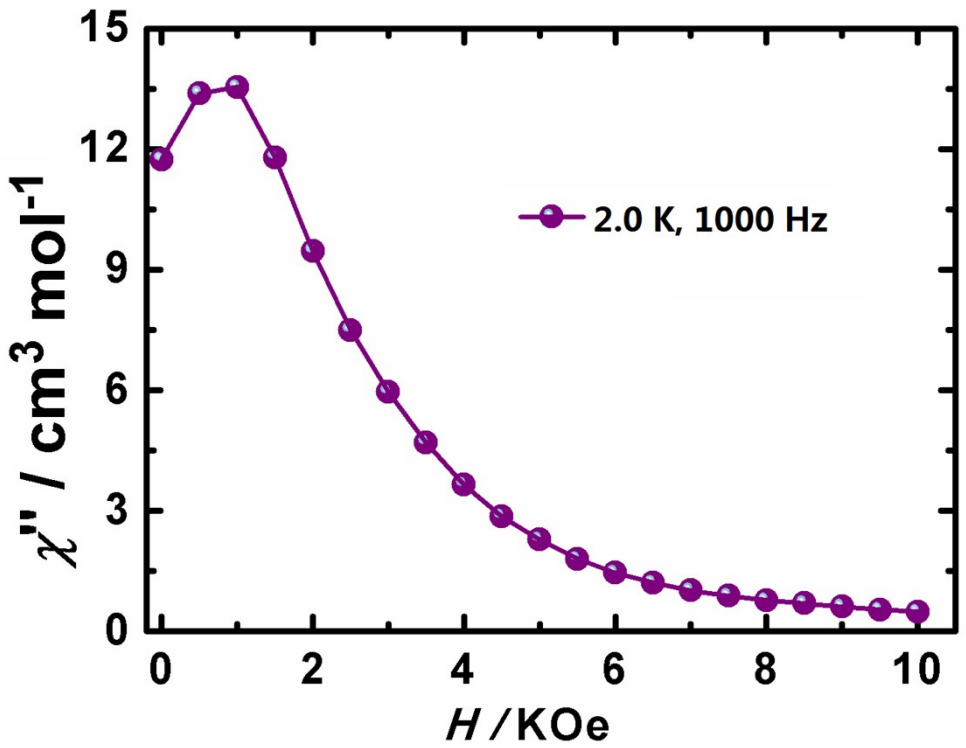

Figure S23 Field dependence of the χ'' product, *ac* susceptibility of **1** at 1000 Hz and 2 K.

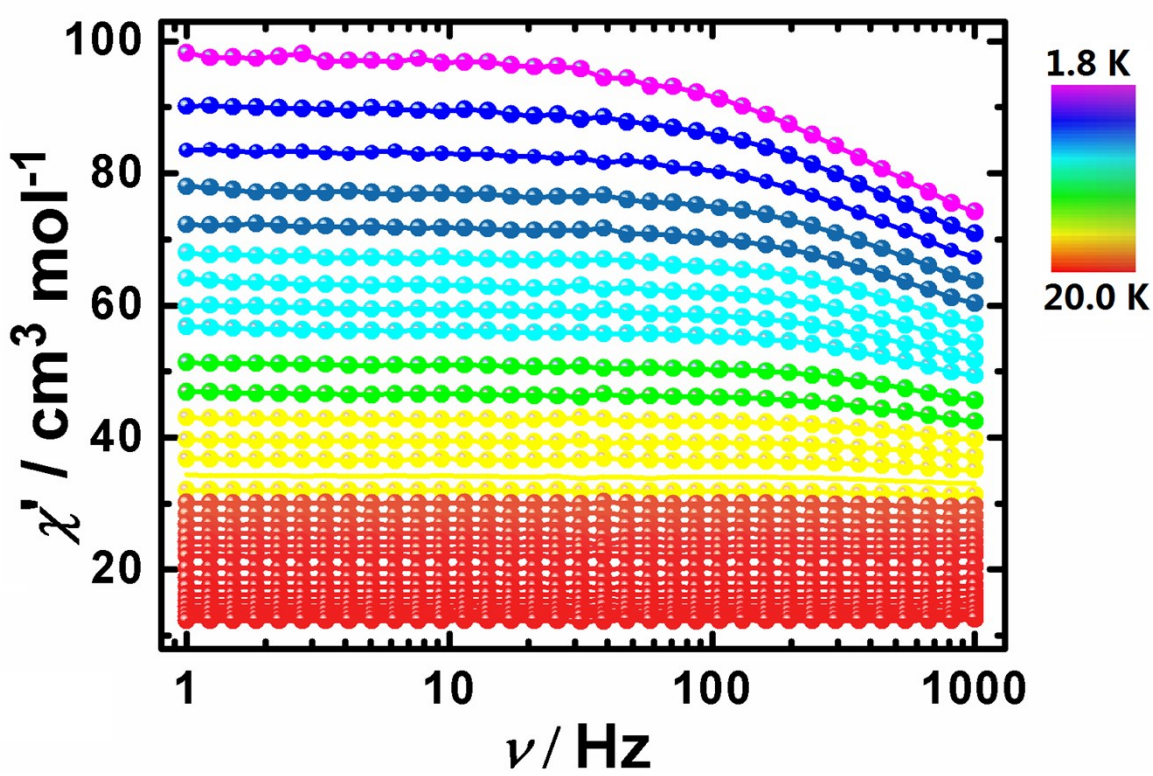

Figure S24 Frequency dependence of the χ' product, *ac* susceptibilities under 1.0 kOe *dc* field for **1**.

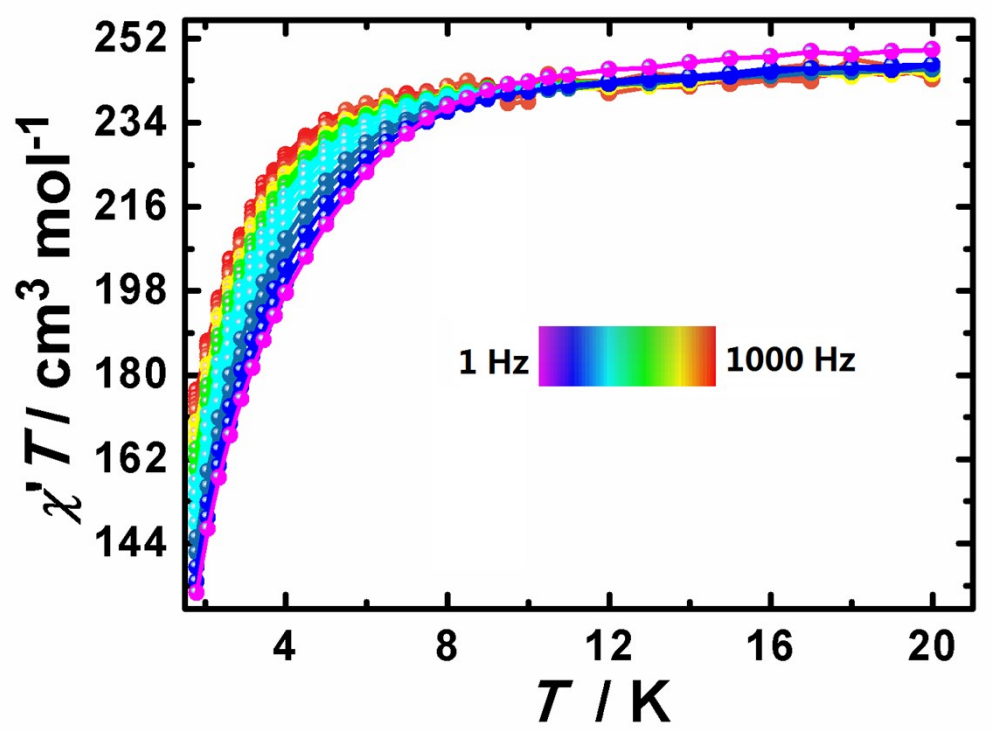

Figure S25 Frequency dependence of the $\chi'T$ product, *ac* susceptibilities under 1.0 kOe *dc* field for **1**.

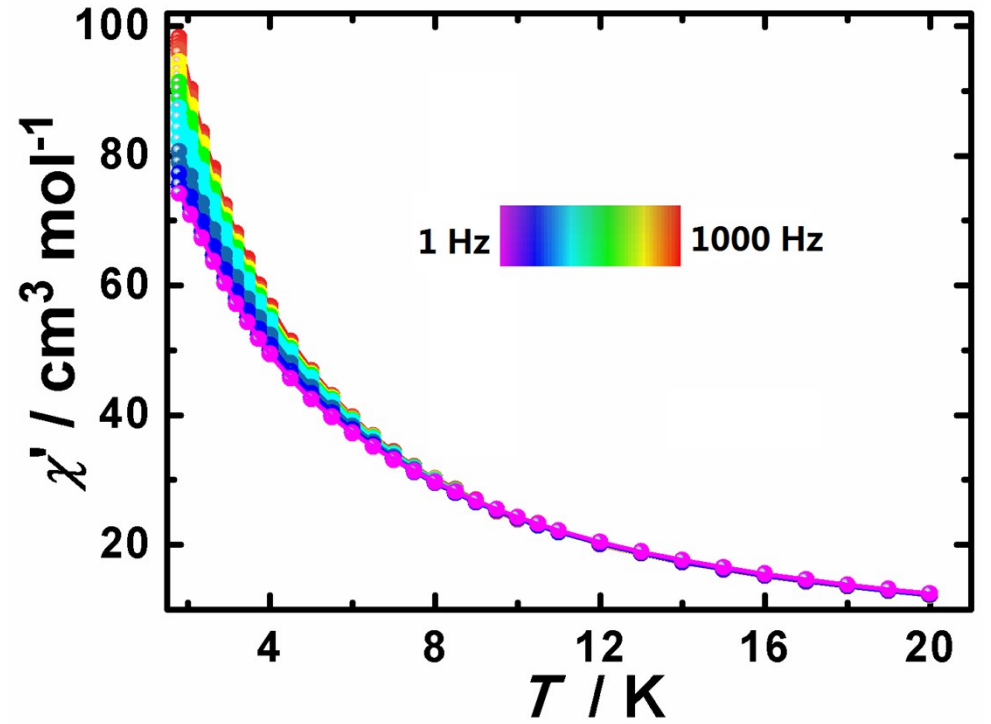

Figure S26 Temperature dependence of the χ' product, *ac* susceptibilities under 1.0 kOe *dc* field for **1**.

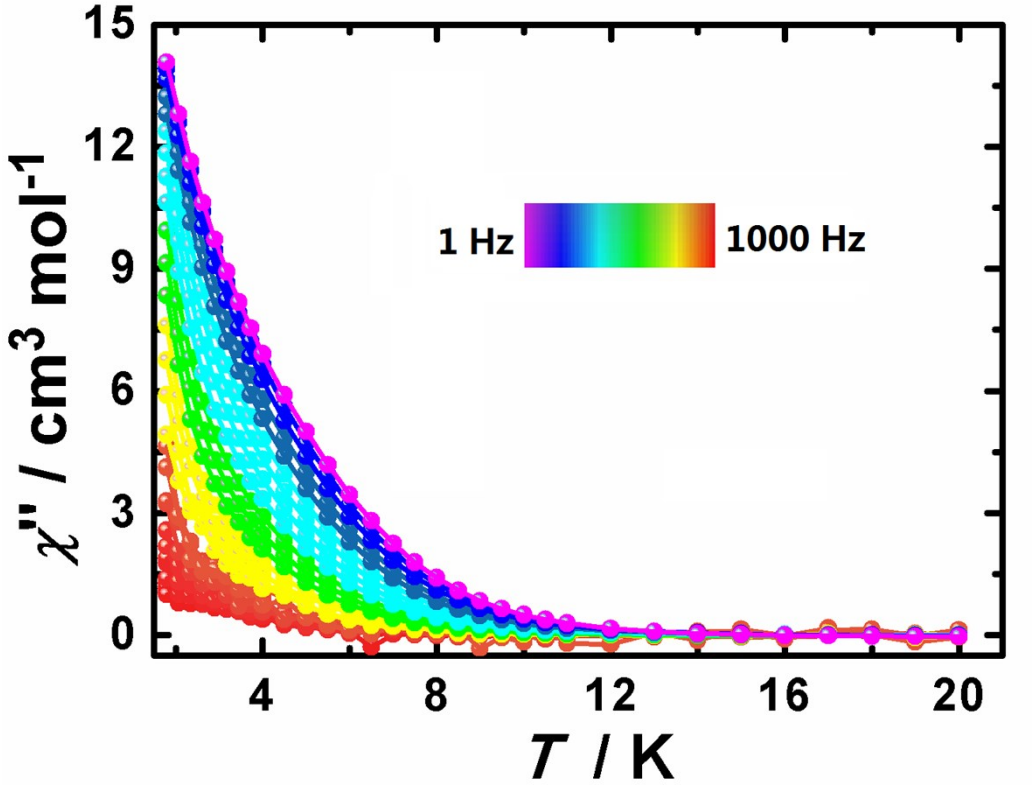

Figure S27 Temperature dependence of the χ'' product, *ac* susceptibility under 1.0 kOe *dc* field for **1**.

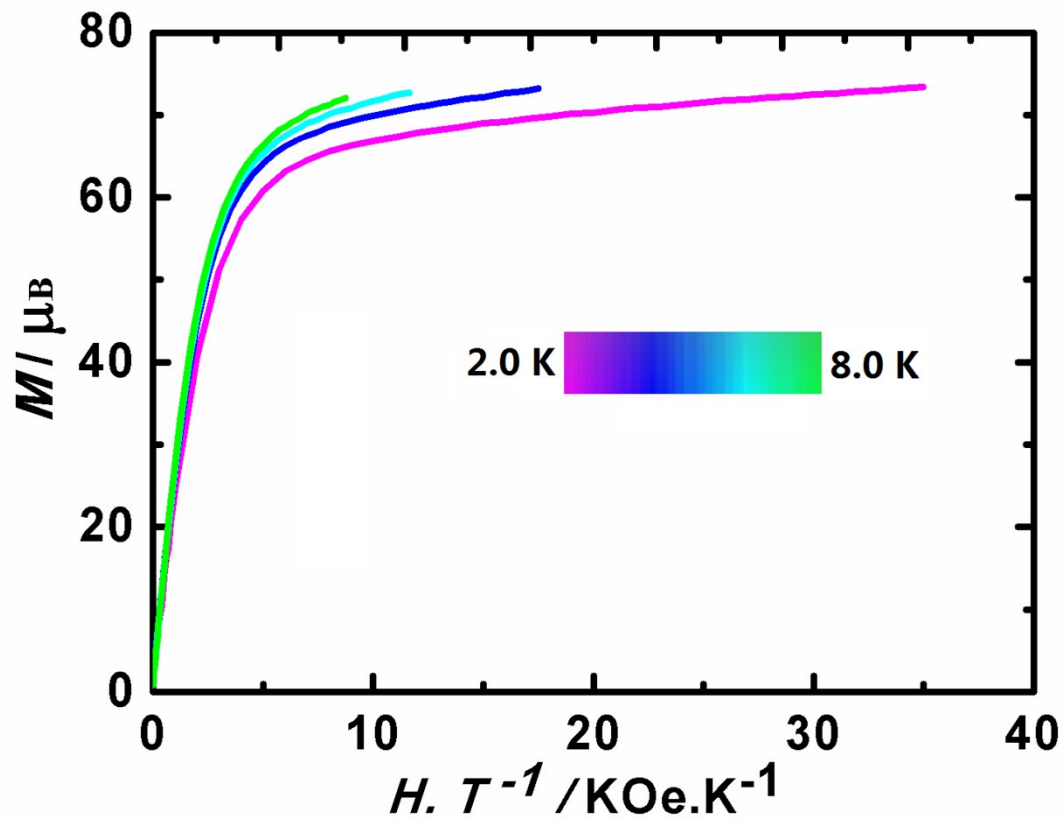

Figure S28 *M vs. H/T* plot for **2** at temperature range of 2.0 K – 8.0 K.

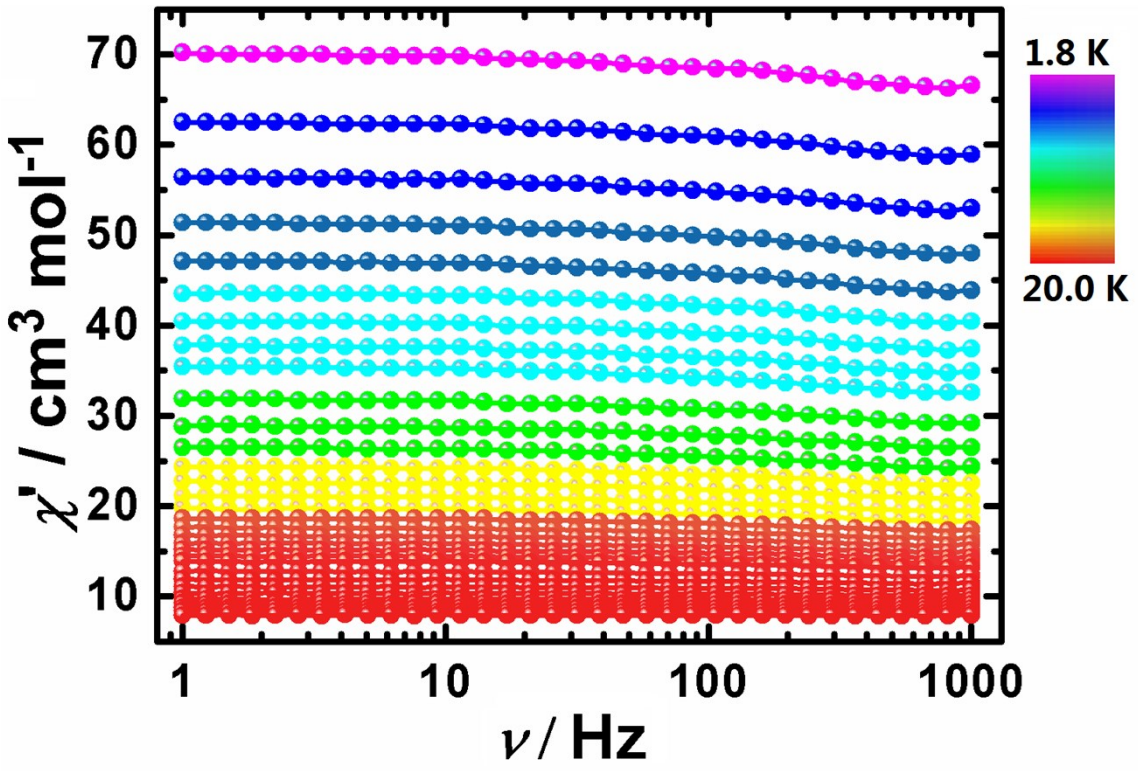

Figure S29 Frequency dependence of the χ' product, *ac* susceptibilities under zero *dc* field for **2**.

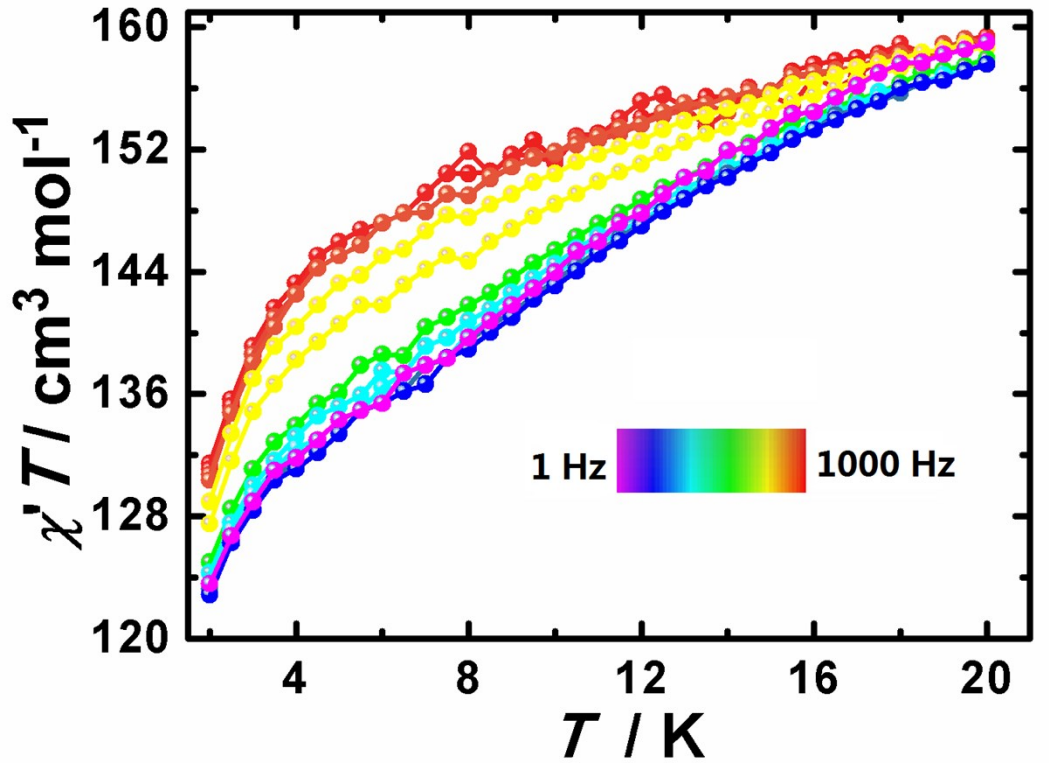

Figure S30 Frequency dependence of the $\chi'T$ product, *ac* susceptibilities under zero *dc* field for **2**.

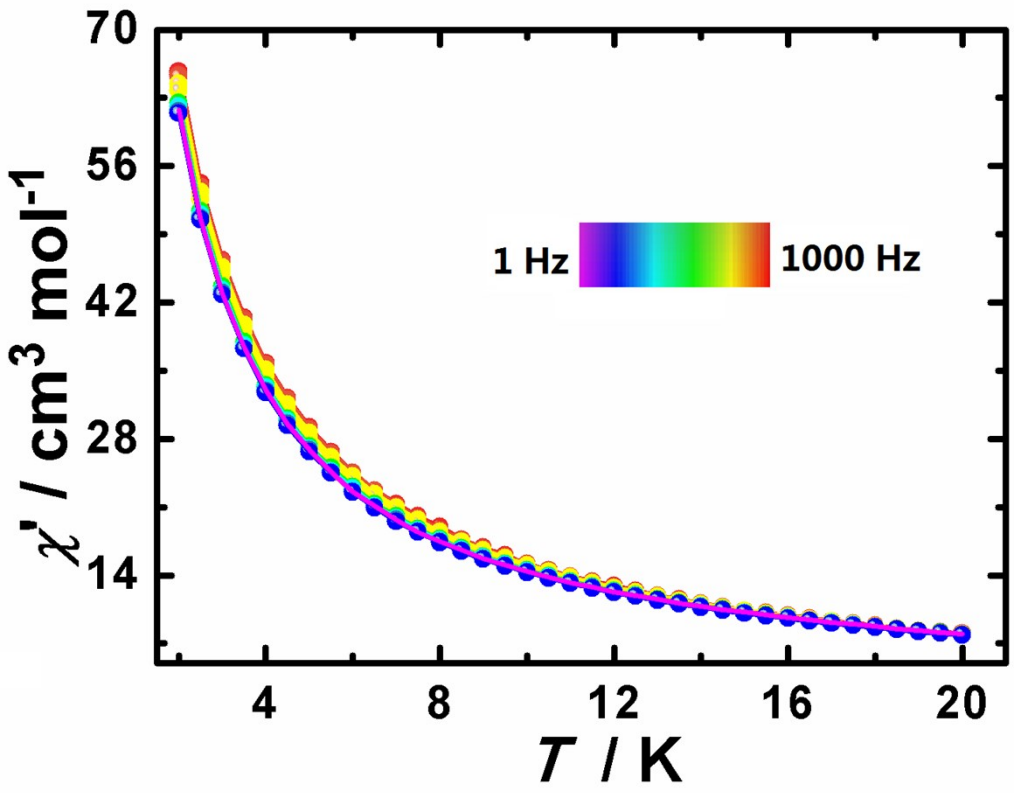

Figure S31 Temperature dependence of the χ' product, *ac* susceptibilities under zero *dc* field for **2**.

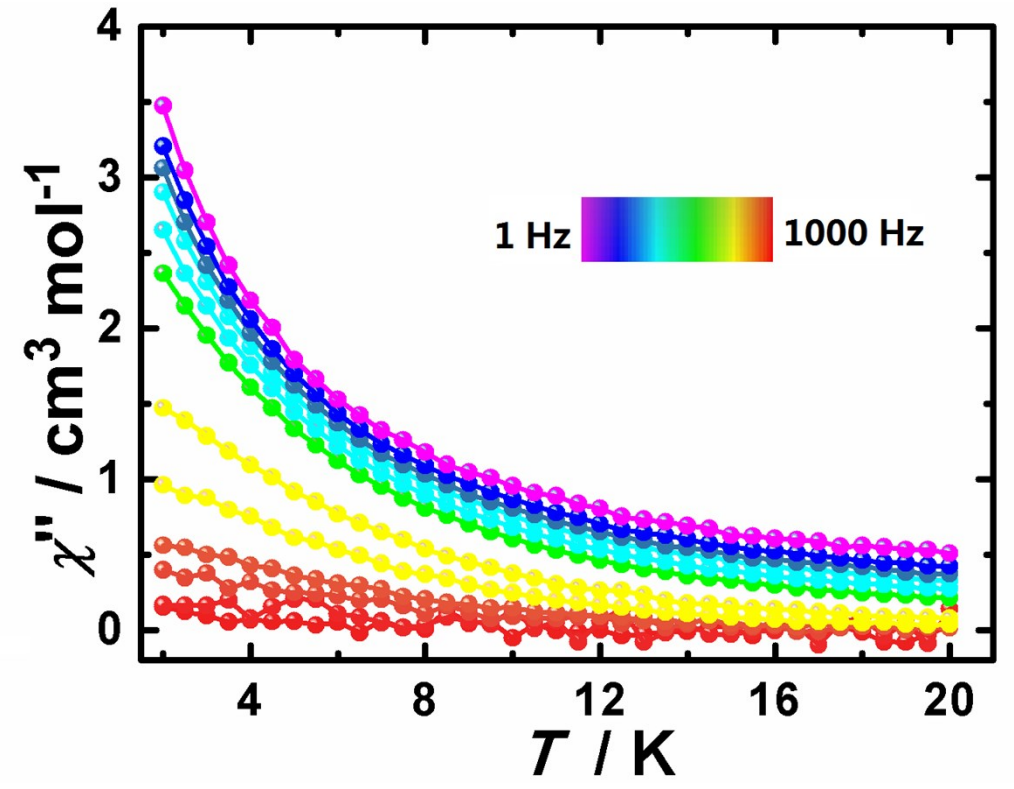

Figure S32 Temperature dependence of the χ'' product, *ac* susceptibility under zero *dc* field for **2**.

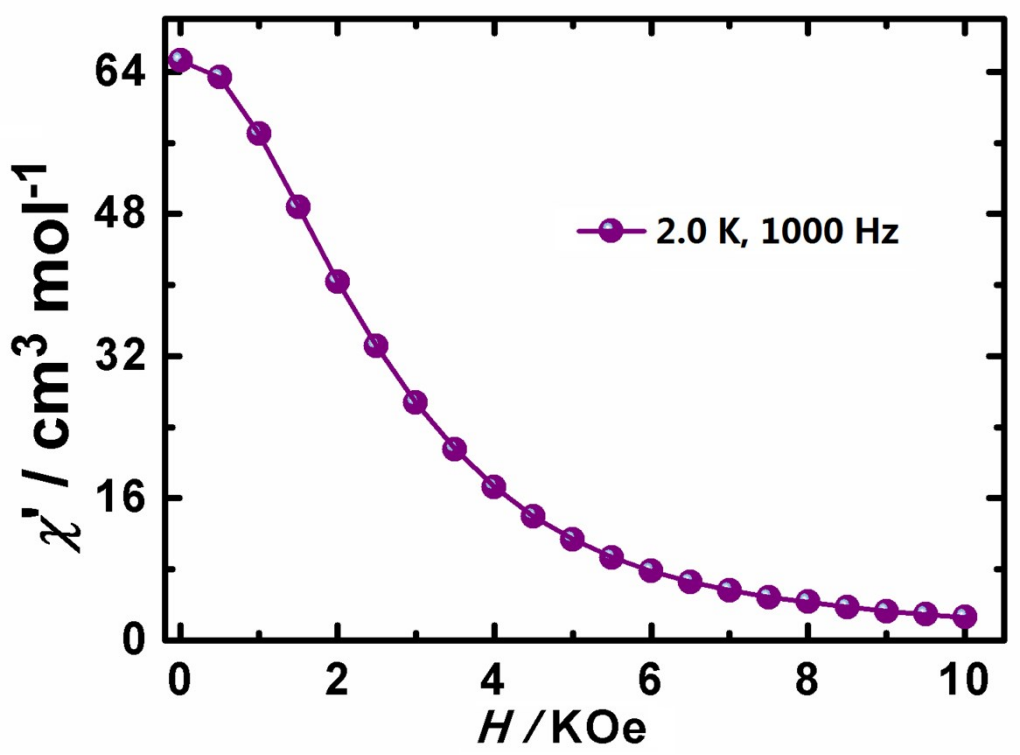

Figure S33 Field dependence of the χ' product, ac susceptibility of **2** at 1000 Hz and 2 K.

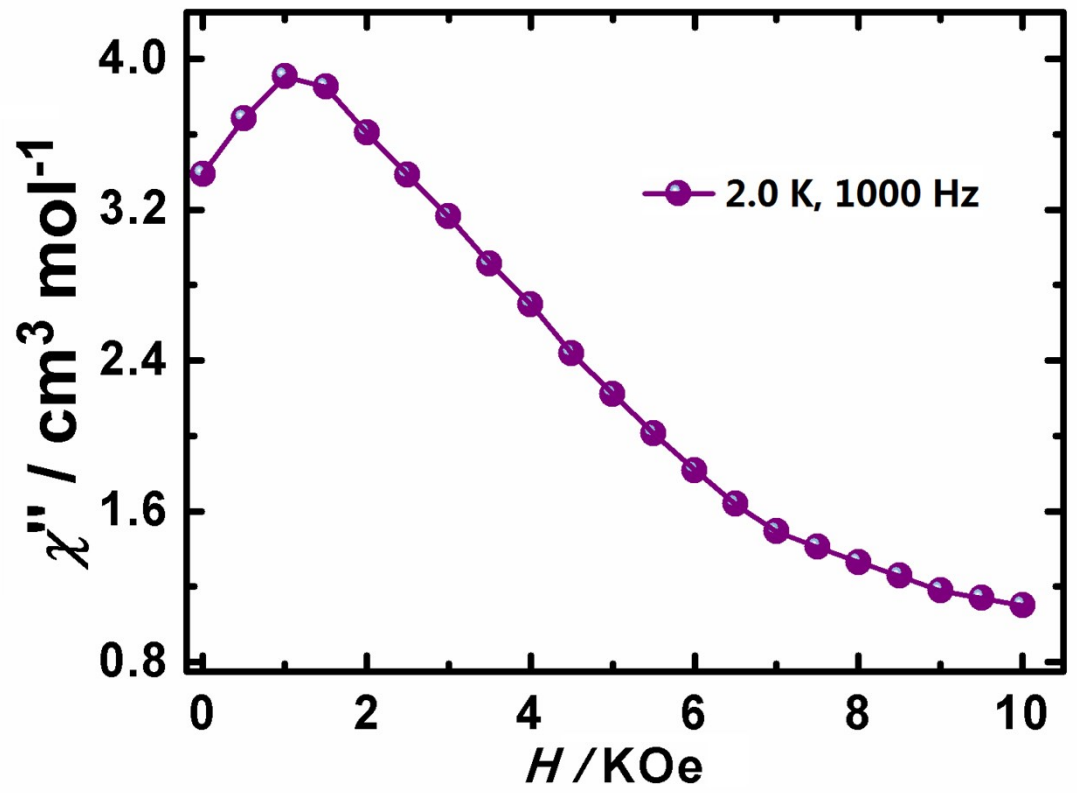

Figure S34 Field dependence of the χ'' product, *ac* susceptibility of **2** at 1000 Hz and 2 K.

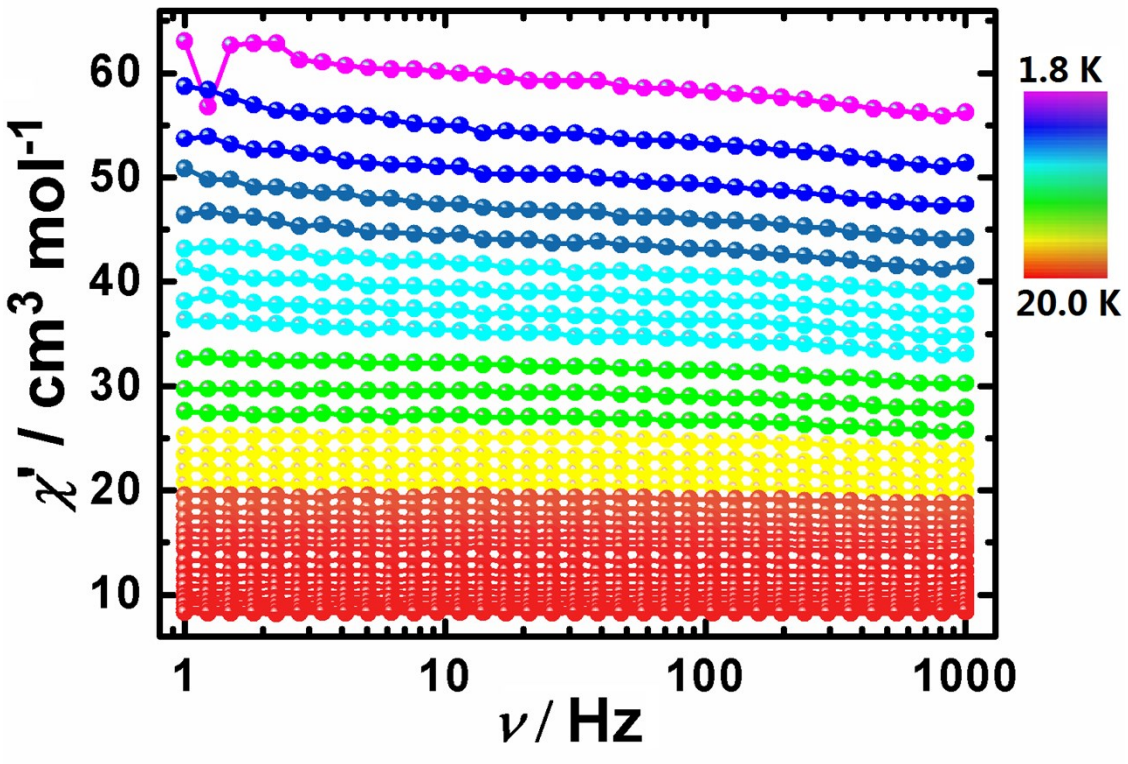

Figure S35 Frequency dependence of the χ' product, *ac* susceptibilities under 1.0 kOe *dc* field for **2**.

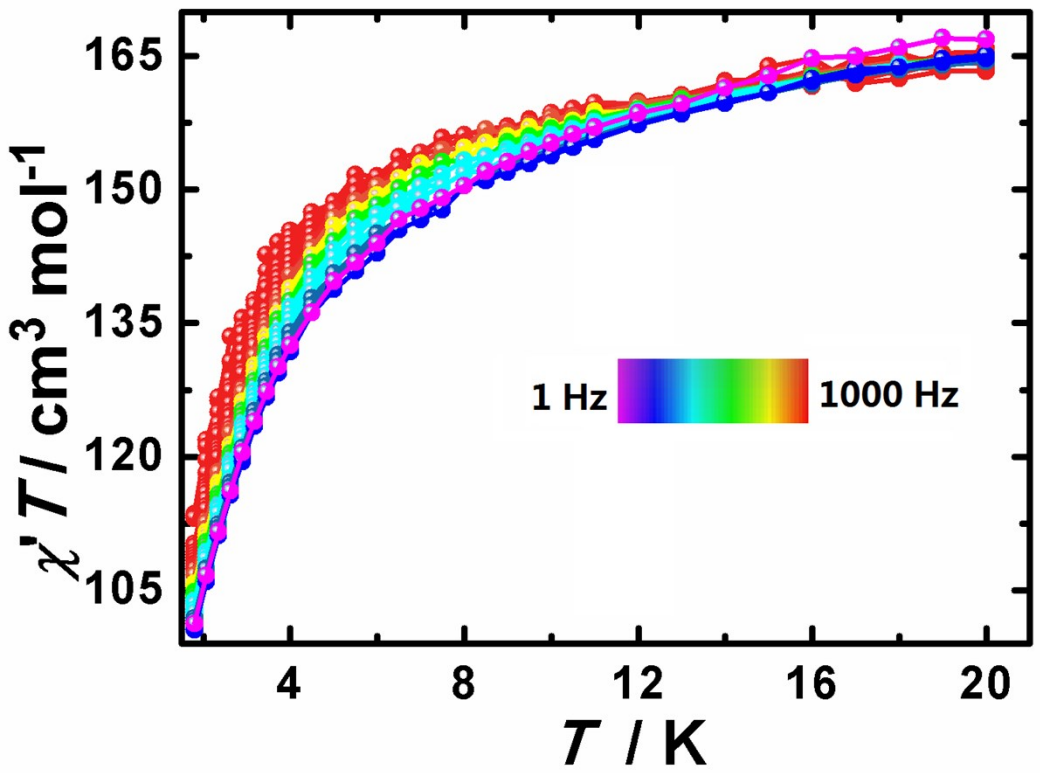

Figure S36 Frequency dependence of the $\chi'T$ product, *ac* susceptibilities under 1.0 kOe *dc* field for **2**.

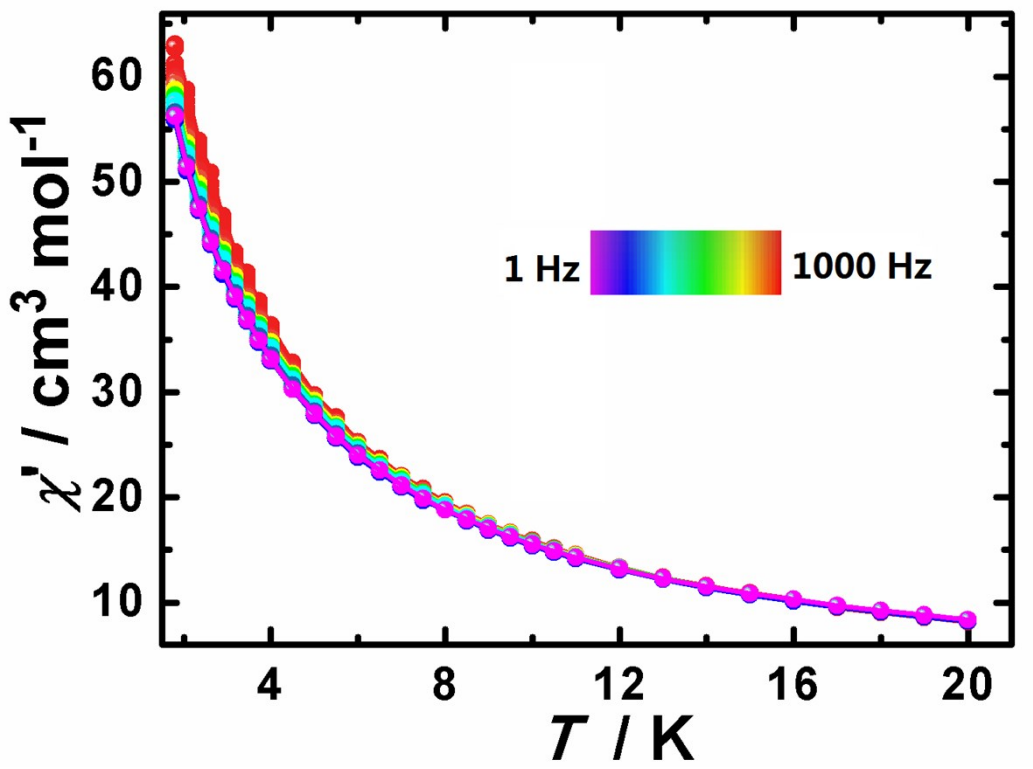

Figure S37 Temperature dependence of the χ' product, *ac* susceptibilities under 1.0 kOe *dc* field for **2**.

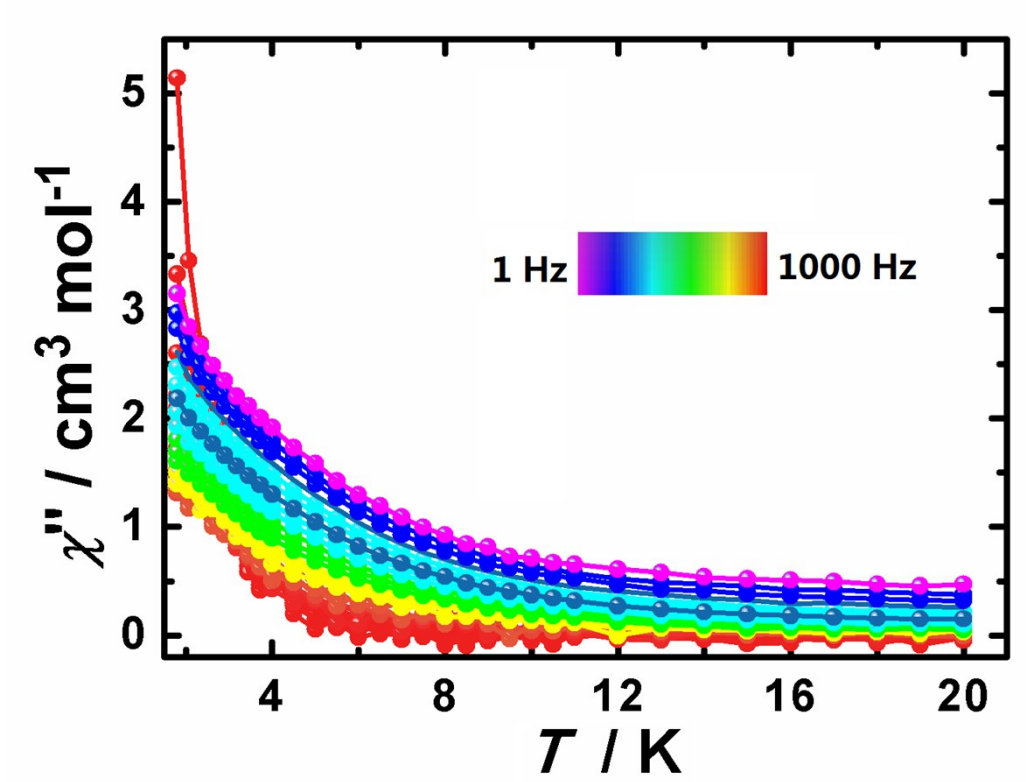

Figure S38 Temperature dependence of the χ'' product, *ac* susceptibility under 1.0 kOe *dc* field for **2**.